4-23-2013

Supramolecular Composite Materials from Cellulose, Chitosan, and Cyclodextrin: Facile Preparation and Their Selective Inclusion Complex Formation with Endocrine Disruptors

Simon Duri
Marquette University, simon.duri@marquette.edu

Chieu D. Tran
Marquette University, chieu.tran@marquette.edu

Accepted version. *Langmuir*, Vol. 29, No. 16 (April 23, 2013): 5037-5049. DOI.

Supramolecular Composite Materials from Cellulose, Chitosan, and Cyclodextrin: Facile Preparation and Their Selective Inclusion Complex Formation with Endocrine Disruptors

Simon Duri
Department of Chemistry, Marquette University, Milwaukee, WI
Chieu D. Tran
Department of Chemistry, Marquette University, Milwaukee, WI

Abstract: We have successfully developed a simple and one step method to prepare high performance supramolecular polysaccharide composites from cellulose (CEL), chitosan (CS) and (2,3,6-tri-O-acetyl)-α-, β- and γ-cyclodextrin (α-, β- and γ-TCD). In this method, [$BMIm^+Cl^-$], an ionic liquid (IL), was used as a solvent to dissolve and prepare the composites. Since majority (>88%) of the IL used was recovered for reuse, the method is

Langmuir, Vol 29, No. 16 (April 23, 2013): pg. 5037-5049. DOI.

recyclable. XRD, FT-IR, NIR and SEM were used to monitor the dissolution process and to confirm that the polysaccharides were regenerated without any chemical modifications. It was found that unique properties of each component including superior mechanical properties (from CEL), excellent adsorbent for pollutants and toxins (from CS) and size/structure selectivity through inclusion complex formation (from TCDs) remain intact in the composites. Specifically, results from kinetics and adsorption isotherms show that while CS-based composites can effectively adsorb the endocrine disruptors (polychlrophenols, bisphenol-A), its adsorption is independent on the size and structure of the analytes. Conversely, the adsorption by γ-TCD-based composites exhibits strong dependency on size and structure of the analytes. For example, while all three TCD-based composites (i.e., α-, β- and γ-TCD) can effectively adsorb 2-, 3- and 4-chlorophenol, only γ-TCD-based composite can adsorb analytes with bulky groups including 3,4-dichloro- and 2,4,5-trichlorophenol. Furthermore, equilibrium sorption capacities for the analytes with bulky groups by γ-TCD-based composite are much higher than those by CS-based composites. Together, these results indicate that γ-TCD-based composite with its relatively larger cavity size can readily form inclusion complexes with analytes with bulky groups, and through inclusion complex formation, it can strongly adsorb much more analytes and with size/structure selectivity compared to CS-based composites which can adsorb the analyte only by surface adsorption.

1. Introduction

Supramolecular composite material is an organized, complex entity that is created from the association of two or more chemical species held together by intermolecular forces.[1–5] Its structure is the result of not only additive but also cooperative interactions, and its properties are often better than the sum of the properties of each individual component[1–3]. Supramolecular composite materials containing marcrocyclic polysaccharides such as cyclodextrins (CDs) are of particular interest because CD ((α-, β- and γ-CD) are known to form selective inclusion complexes with a variety of different compounds with different sizes and shapes.[4–6] To be able to fully and practically utilize properties of CD-based supramolecular composite material, it is necessary for the materials to be readily fabricated in solid form (film and/or particle) in which encapsulated CDs fully retain their unique properties. CDs are highly soluble in water, and cannot be processed in film because of its poor mechanical and rheological strength. As a consequence, it is often necessary to chemically react and/or graft CD onto man-made polymers to increase its mechanical strength so that the resultant materials can be processed into solid thin film and/or particles.[7–10] CD-based materials synthesized by these

Langmuir, Vol 29, No. 16 (April 23, 2013): pg. 5037-5049. DOI.

methods have been reported. Unfortunately, in spite of their potentials, practical applications of such materials are rather limited because in addition to complexity of reactions used in the synthesis which are limited to persons with synthetic expertise, method used may also alter and/or lessen desired properties of CDs.[7,8,11,12] It is, therefore, desirable to improve the mechanical strength of CD-based supramolecular material so that it can be fabricated into a solid film (or particles) not by chemical modification with synthetic chemicals and/or polymers but rather by use of naturally occurring polysaccharides such as cellulose and/or chitosan which are structurally similar to CDs.

Cellulose (CEL) and chitosan (CS) are two of the most abundant biorenewable biopolymers on the earth. The latter is derived by N-deacetylation of chitin which is the second most abundant naturally occurring polysaccharide found in the exoskeletons of crustaceans such as crabs and shrimp. In these polysaccharides, an extensive network of intra- and inter-hydrogen bonds enables them to adopt an ordered structure. While such structure is responsible for CEL to have superior mechanical strength and CS to exhibit remarkable properties such as hemostasis, wound healing, bactericide and fungicide, drug delivery and adsorbent for organic and inorganic pollutants, it also makes them insoluble in most solvents[9,10,13–18]. This is rather unfortunate because with their superior mechanical strength and unique properties, CEL and CS would be excellent supporting polymer for CD. It is expected that the resulting [CEL and/or CS+CD] composite would have properties that are a combination of those of all of its components. That is, it may have superior mechanical strength (from CEL), can stop bleeding, heal wound, kill bacteria, deliver drugs (from CS) and selectively form inclusion complexes with a wide variety of compounds of different types, sizes and shapes (from CDs). Unfortunately, to date, such supermolecules have not been realized because of lack of a suitable solvent which can dissolve all three compounds. The difficulty stems from the fact that while CDs are water soluble CEL and CS are insoluble in most solvents. Furthermore, there is not a solvent or system of solvents which can dissolve all three CEL, CS and CD.

Considerable efforts have been made in the last few years to find suitable solvents for CEL and CS, and several solvent systems

Langmuir, Vol 29, No. 16 (April 23, 2013): pg. 5037-5049. DOI.

have been reported.[19–20] For example, high temperature and strong exotic solvents such as methylmorpholine-N-oxide, dimethylthexylsilyl chloride or LiCl in dimethylacetamide (DMAc) are needed to dissolve CEL whereas an acid such as acetic acid is required to protonate amino groups of CS so that it can be dissolved in water [6–29]. These methods are undesirable because they are based on the use of corrosive and volatile solvents, require high temperature and suffer from side reactions and impurities which may lead to changes in structure and properties of the polysaccharides. More importantly, it is not possible to use a single solvent or system of solvents to dissolve both CEL and CS. A new method which can effectively *dissolve all three CS, CEL and CD,* not at high temperature and not by corrosive and volatile solvents but rather by recyclable "green" solvent is particularly needed. This is because such method would facilitate preparation of [CS+CD] and [CEL+CD] composite materials which are not only biocompatible but also have combined properties of its components.

Recently, we have developed a new method which can offer a solution for this problem.[21] In this method, we (1) exploited advantages of a simple ionic liquid, butyl methylimmidazolium chloride ($BMIm^+Cl^-$), a green solvent,[22–25] to develop an innovative, simple, pollution-free method to dissolve not only CS but also other polysaccharides including CEL without using any acid or base, thereby avoiding any possible chemical or physical changes, and (2) used only naturally occurring biopolymers such as CEL as support materials to strengthen structure and expand utilities while keeping the biodegradable, biocompatible and anti-infective and drug carrier properties of CS-based materials intact. Using this method, we have successfully synthesized composite materials containing CEL and CS with different compositions. As expected, the composite materials obtained were found to have combined advantages of their components, namely superior chemical stability and mechanical stability (from CEL) and excellent antimicrobial properties (from CS). The [CEL+CS] composite materials inhibit growth of a wider range of bacteria than other CS-based materials prepared by conventional methods. Specifically, it was found that over a 24 hr period, the composite materials substantially inhibited growth of bacteria such as *Methicillin Resistant Staphylococcus Aureus* (MRSA), *Vancomycin Resistant Enterococcus* (VRE)*, S. aureus* and *E. coli.* [21]

Langmuir, Vol 29, No. 16 (April 23, 2013): pg. 5037-5049. DOI.

The information presented is indeed provocative and clearly indicate that it is possible to use this simple, one-step process without any chemical modification to synthesize novel supramolecular composite materials from CEL, CS and CDs. Based on results of our previous work on the [CEL+CS] composites[21], it is expected that the [CEL and/or CS+CD] composite materials may possess all properties of their components, namely mechanical strength (from CEL), excellent adsorbent for toxins and pollutants (from CS) and selectively form inclusion complexes with substrates of different sizes and shapes (from CDs). Such considerations prompted us to initiate this study which aims to hasten the breakthrough by using the method which we have developed recently to synthesize novel supramolecular composite materials from CEL, CS and CDs. Results on the synthesis, spectroscopic characterization and applications of the composite materials for removal of organic pollutants such as endocrine disruptors are reported herein.

2. Experimental Section

2.1. Chemicals

Cellulose (microcrystalline powder) and chitosan (MW ≈310-375kDa) were purchased from Sigma-Aldrich (Milwaukee, WI) and used as received. [$BMIm^+Cl^-$] was synthesized from freshly vacuum distilled 1-methylimidazole and 1-chlorobutane (Alfa Aesar, Ward Hill, MA) using procedure previously used in our lab.[21,26] 2-chlorophenol (2 Cl-Ph), 3 chlorophenol (3 Cl-Ph), 4-chlorophenol (4 Cl-Ph), 3,4 dichlorophenol (3,4 di Cl-Ph), 2,4,5 trichlorophenol (2,4,5 tri Cl-Ph) and bisphenol A (BPA) were from Sigma Aldrich (Milwaukee, WI). Heptakis(2,3,6-tri-O-acetyl)-β-cyclodextrin (β-TCD) (TCI America, Portland, OR), hexakis(2,3,6-tri-O-acetyl)-α-cyclodextrin (α-TCD) and octakis(2,3,6-tri-O-acetyl)-γ-cyclodextrin (γ-TCD) (Cyclodextrin-Shop, The Netherlands) were used as received. See Scheme 1 for structures of compounds used in this study.

Langmuir, Vol 29, No. 16 (April 23, 2013): pg. 5037-5049. DOI.

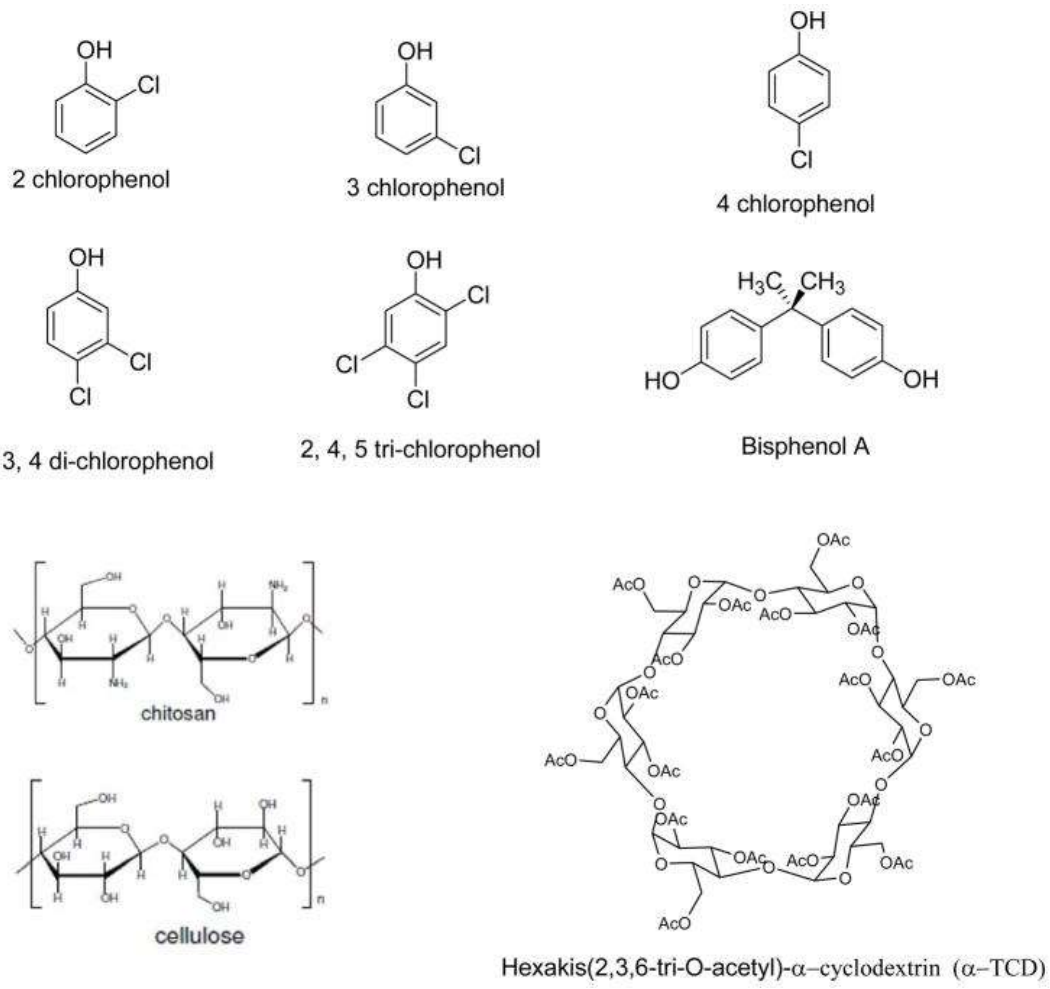

Scheme 1. Structure of Compounds used

2.2. Instrumentation

Elemental analysis was carried out by Midwest Microlab, LLC (Indianapolis, IN). ^{1}H NMR spectra were taken on a VNMRS 400 spectrometer. Near-infrared (NIR) spectra were recorded on a home-built NIR spectrometer.[27] FT-IR spectra were measured on a PerkinElmer 100 spectrometer at 2 cm^{-1} resolution with either KBr or by a ZnSe single reflection ATR accessory (Pike Miracle ATR). X-ray diffraction (XRD) measurements were taken on a Rigaku MiniFlex II diffractometer utilizing the Ni filtered Cu Kα radiation (1.54059Å).[28] Scanning electron microscopic images of surface and cross section of the composite materials were taken under vacuum with an accelerated voltage of 3 kV using Hitachi S4800 scanning electron microscope

(SEM). Tensile strength measurements were performed on an Instron 5500R Tensile Tester.

2.3. Preparation of [CEL+TCD] and [CS+TCD] composite films

[CEL+α-TCD, β-TCD and γ-TCD] and [CS+α-TCD, β-TCD and γ-TCD] composite materials were synthesized using a procedure similar to that previously developed in our laboratory for the synthesis of CEL, CS and [CEL+CS].[21] Essentially, as shown in Scheme 2, an ionic liquid, [$BMIm^+$ Cl^-], was used as a solvent to dissolve CEL, CS, α-TCD, β-TCD and γ-TCD. Dissolution was performed at 100°C and under Ar or N_2 atmosphere. All polysaccharides were added in portions of approximately 1 wt% of the ionic liquid. Succeeding portions were only added after the previous addition had completely dissolved until the desired concentration has been reached. For composite films, the components were dissolved one after the other, with CEL (or CS) being dissolved first and TCDs last. Using this procedure, solutions of CEL (containing up to 10% w/w (of IL)), CS (up to 4% w/w) and composite solutions containing CEL (or CS) and α-TCD, β-TCD or γ-TCD with various proportions were prepared in about 6–8 hours.

Langmuir, Vol 29, No. 16 (April 23, 2013): pg. 5037-5049. DOI.

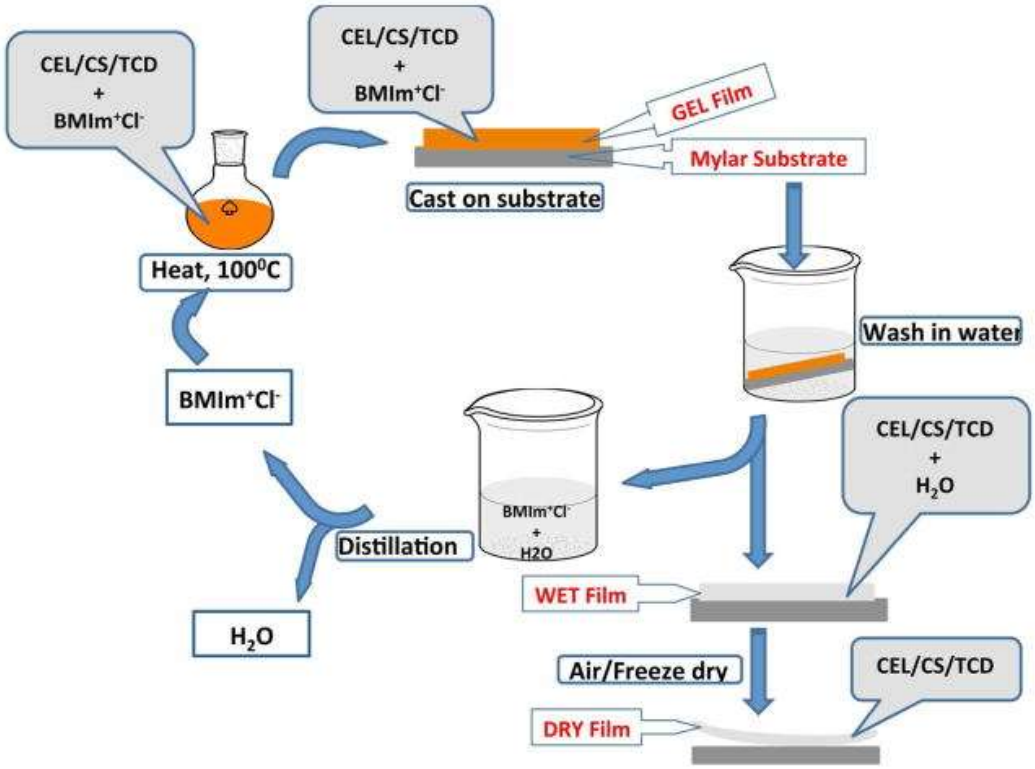

Scheme 2. Procedure used to prepare the cellulose-chitosan-TCD composite materials

Upon complete dissolution, the homogeneous solutions of the polysaccharides in [$BMIm^+Cl^-$] were cast on glass slides or Mylar sheets using a RDS stainless steel coating rod with appropriate size (RDS Specialties, Webster, NY) to produce thin films with different compositions and concentrations of CEL (or CS) with α-TCD, β-TCD or γ-TCD. If necessary, thicker composite materials can be obtained by casting the solutions onto PTFE moulds of the desired thickness. They were then kept at room temperature for 24 hours to allow the solutions to undergo gelation to yield **GEL Films**. The [$BMIm^+$ Cl^-] remaining in the film was then removed by washing the films in deionized water for about 3 days to yield **WET Films**. During this period, the washing water was constantly replaced with fresh deionized water to maximize the removal of the ionic liquid. The [$BMIm^+$ Cl^-] used was recovered from the washed aqueous solution by distillation. It was found that at least 88% of [$BMIm^+Cl^-$] was recovered for reuse. The regenerated composite materials were lyophilized overnight to remove water, yielding dried porous composite films (**DRY films**).

Langmuir, Vol 29, No. 16 (April 23, 2013): pg. 5037-5049. DOI.

2.4. Procedure used to measure kinetics of adsorption

Two matching cuvettes were used for all adsorption measurements, one for adsorption of the pollutant by the composite and the other as the blank (blank 1). Photograph of the two cells is shown in figure SI-1 (of the Supporting Information). The samples (about 0.02g of dry film of the composite material) was washed thoroughly in water prior to the adsorption experiments to further insure that [$BMIm^+$ Cl^-] was completely removed because absorption of any residual IL may interfere with that of polychlorophenols or BPA. To wash the samples, the weighed composite materials were placed in a thin cell fabricated from PTFE whose windows were covered by two PTFE meshes. The meshes ensured free circulation of water through the material during the washing process. The PTFE mould containing the samples was placed in a 2L beaker which was filled with de-ionized water and was stirred at room temperature for 24 hours. During this time, absorbance of washed water was monitored at 214 and 287nm to determine the presence of any [$BMIm^+$ Cl^-]. The water in the beaker was replaced with fresh de-ionized water every 4 hours.

After 24 hours, the composite material was taken out of the water and placed into the sample cuvette (cell in the right of the photograph shown in Fig SI-1). Both sample and blank cells were stirred using a small magnetic spin bar during the measurement. In order to prevent damage to the sample by the magnetic spin bar and to maximize the circulation of the solution during measurement, the samples were sandwiched between two PTFE meshes. Specifically, a piece of PTFE mesh was placed at the bottom of the spectrophotometric cell. The washed film sample was laid flat on top of the PTFE mesh. Another piece of PTFE mesh was placed on top of the sample and finally the small magnetic spin bar was placed on top of the second mesh. The blank cell, shown on the left of the photograph in Figure SI-1, had the same contents as the sample cell but without the composite material. Exactly 2.70mL of 1.55×10^{-4}M aqueous solution of polychlorophenol or BPA was added to both sample and blank cell. A second blank cell (blank 2) was also employed. This blank cell 2 had the same contents as the sample cell (i.e., PTFE mesh, composite film, PTFT mesh and magnetic spin bar) but without the pollutant. Any adsorption of the pollutants by the cell content (PTFE

Langmuir, Vol 29, No. 16 (April 23, 2013): pg. 5037-5049. DOI.

mesh, magnetic spin bar) and not by the composite materials was corrected by the signal of blank 1. Blank 2 provided information on any possible interference of absorption of pollutant by leakage of residual IL from the composite film. Measurements were carried out on a Perkin Elmer Lambda 35 UV/VIS spectrometer set to the appropriate wavelength for each pollutant, i.e., 274nm for 2- and 3-chlorophenol, 280nm for 4-chlorophenol, 282nm and 289nm for 3,4-dichloro- and 2,4,5-trichlorophenol, respectively, and 276nm for bisphenol A. Measurements were taken at 10 minute intervals during the first 2 hours and 20 minute intervals after 2 hours. After each measurement, the cell was returned to a magnetic stirrer for continuous stirring. Reported values were the difference between the sample signals and those of blank 1 and blank2. However, it was found that signals measured by both blank cells were negligible within experimental error.

2.5. Procedure used to measure equilibrium sorption isotherms

Batch sorption experiments were carried out in 50mL stoppered vials containing 10mL of the pollutant solution of known initial concentration. A weighed amount (0.1g) of the composite material was added to the solution. The samples were agitated at 250 rpm in a shaking water bath at 25°C for 72 hours. The residual amount of pollutant in each flask was analyzed by UV/Vis spectrophotometry. The amount of pollutant adsorbed onto the composite material was calculated using the following mass balance equation:

$$q_e = \frac{(C_i - C_e)V}{m} \quad [1]$$

where q_e (mg/g) is the equilibrium sorption capacity, C_i and C_e (mg/L) are the initial and final pollutant concentrations respectively. V (L) is the volume of the solution and m (g) is the weight of the composite film material.

Detailed information on analysis of Kinetic Data and equilibrium sorption isotherms can be found in the Supporting Information.

3. Results and Discussion

3.1. Synthesis and Characterization of CEL/CS +α-TCD, β-TCD and γ-TCD Composite Materials

The CS used in this study was specified by the manufacturer (Sigma-Aldrich) as having a degree of deacetylation (DA) value of 75%. As will be described below, because unique properties of CS including its ability to adsorb pollutants are due to its amino groups, experiments were performed to determine its DA value. Two different methods, FT-IR and ^{1}H NMR, were employed for the determination[30–35]. For FT-IR method, the spectra were taken at 2 cm^{-1} resolution. The CS sample was vacuum dried at 50°C for 2 days. A small amount of the dried sample was then ground in KBr and pressed into a pellet for FT-IR measurements. Four KBr pellets were prepared and their spectra were recorded. Degree of deacetylation (DA) was calculated from the four spectra, and average value is reported together with standard deviation. The DA value was calculated based on the following equation:[30–31]

$$DA(\%) = 100 - [(A_{1655}/A_{3450}) * 100/1.33] \quad [2]$$

where A_{1655} and A_{3450} are the absorbances at 1655cm^{-1} of the amide C=O and 3450cm^{-1} of the OH band respectively. The factor 1.33 denotes the value of the ratio of A_{1655}/A_{3450} for fully N-acetylated chitosan. A DA% value of 84±2 was found using this method.

For ^{1}H NMR determination, the spectra were taken at 70°C. About 5mg of chitosan sample which was previously vacuum dried at 50°C for 2 days, was dissolved in 0.5mL of 2 wt% DCl/D2O solution at 70°C. The degree of deacetylation (DA) was evaluated from the following equation using the integral intensity, I_{CH3}, of the CH_3 residue of N-acetyl, and the sum of the integral intensities, $I_{H2\text{-}H6}$, of protons 2–6 of the chitosan residue:[35]

Langmuir, Vol 29, No. 16 (April 23, 2013): pg. 5037-5049. DOI.

$$DA(\%) = \left[1 - \left(\frac{1}{3} I_{CH3} / \frac{1}{6} I_{H2-H6}\right)\right] 100 \quad [3]$$

A DA value of 78% was found using this method.

It has been reported that chitosan samples may contain some protein impurities. Accordingly, experiments were carried out to determine any possible protein impurities in the CS sample used in this study. The percentage of proteins impurity (%P) can be calculated from the following equation[36–38]

$$\%P = (\%N - N_T) \times 6.25 \quad [4]$$

where 6.25 corresponds to the theoretical percentage of nitrogen in proteins; %N represents the percentage of nitrogen measured by elemental analysis; N_T represents the theoretical nitrogen content of chitosan sample. It was calculated based on the degree of deacetylation (DA) of chitosan and percentage of nitrogen for fully acetylated chitin and fully deacetylated chitosan (6.89 and 8.69),[36–38] respectively. Using DA values of 84% (from FT-IR) and 78% (from NMR), percentage of protein impurities in CS sample were found to be 1.89% and 1.24%, respectively. When errors associated with elemental analysis and with the determination of DA values by FT-IR and NMR method are taken into account, it can be assumed that these two %P values are the same within experimental errors.

As described in the Experimental Section, [$BMIm^+$ Cl^-] was used as the sole solvent to dissolve CEL, CS and TCD to prepare the [CEL+TCD] and [CS+TCD] composite materials. It is noteworthy to add that [$BMIm^+$ Cl^-] is not the only IL that can dissolve the polysaccharides. Other ILs including ethylmethylimidazolium acetate ($EMIm^+Ac^-$), $BMIm^+Ac^-$ and allylmethylimidazolium chloride ($AMIm^+Cl^-$) are also known to dissolve the polysaccharides as well. [$BMIm^+$ Cl^-] was selected because compared to these ILs it can dissolve relatively higher concentration of the polysaccharides. For example, the solubility of CEL in [$BMIm^+$ Cl^-], [$AMIm^+Cl^-$] [$BMIm^+Ac^-$] and [$EMIm^+Ac^-$] was reported to be 20%, 15%, 12% and 8%,

Langmuir, Vol 29, No. 16 (April 23, 2013): pg. 5037-5049. DOI.

respectively). Furthermore, [BMIm$^+$ Cl$^-$]is relatively cheaper than these ILs because it can easily be synthesized in a one-step process from relatively inexpensive reagents (1-methylimidazole and 1-chlorobutane) whereas other ILs are relatively more expensive as they require more expensive reagents (silver acetate) and two-step synthetic process [29, 39–43].

Since [BMIm$^+$ Cl$^-$] is totally miscible with water, it was removed from the Gel Films of the composites by washing the films with water. Washing water was repeatedly replaced with fresh water until it is confirmed that there was no ILs in the washed water (by monitoring UV absorption of the IL at 214nm and 287nm). The IL used was recovered by distilling the washed aqueous solution (the IL remained because it is not volatile). The recovered [BMIm$^+$Cl$^-$] was dried under vacuum at 70°C overnight before reuse. *It was found that at least 88% of [BMIm$^+$Cl$^-$] was recovered for reuse*. ***As such, the method developed here is recyclable because [BMIm$^+$Cl$^-$] is the only solvent used in the preparation and majority of it was recovered for reuse.***

The dissolution of the polysaccharides, for example, CS and TCD, in [BMIm$^+$Cl$^-$] ionic liquid and their regeneration in the composite materials was followed and studied by powder X-ray diffraction (XRD). Figure 1 shows the XRD spectra of the [CS+α-TCD], [CS+β-TCD] and [CS+γ-TCD] composites at various stages of preparation. Difference among XRD spectra of the α-, β- and γ-TCD materials (red curves in 1A, B and C, respectively) seems to indicate that these starting cyclodextrin materials have different structural morphologies. While the XRD spectrum of the β-TCD powder is consistent with a highly crystalline structure, the XRD spectra of α-TCD and γ-TCD seem to suggest that these CDs have an amorphous structure[2]. The XRD spectra of [BMIm$^+$Cl$^-$] (black curves) and the gel films (purple curves) were measured to determine the dissolution of the CS and TCDs in the ionic liquid. As illustrated, the XRD spectra of the gel films are similar to that of [BMIm$^+$Cl$^-$], and do not exhibit any of the CS or TCD diffraction peaks. The absence of the XRD peaks of CS and TCDs and the similarity between the spectra of the gel films to that of the [BMIm$^+$Cl$^-$] clearly indicate that [BMIm$^+$Cl$^-$] completely dissolved CS and TCDs. The XRD spectra of the regenerated composite films (Dry films) are also shown as blue curves in figure 1. As expected, the XRD

Langmuir, Vol 29, No. 16 (April 23, 2013): pg. 5037-5049. DOI.

spectra of the 50:50 CS:α-TCD, 50:50 CS:β-TCD and 50:50 CS:γ-TCD regenerated composite films exhibit XRD peaks which can be attributed to those of α-TCD, β-TCD and γ-TCD respectively.

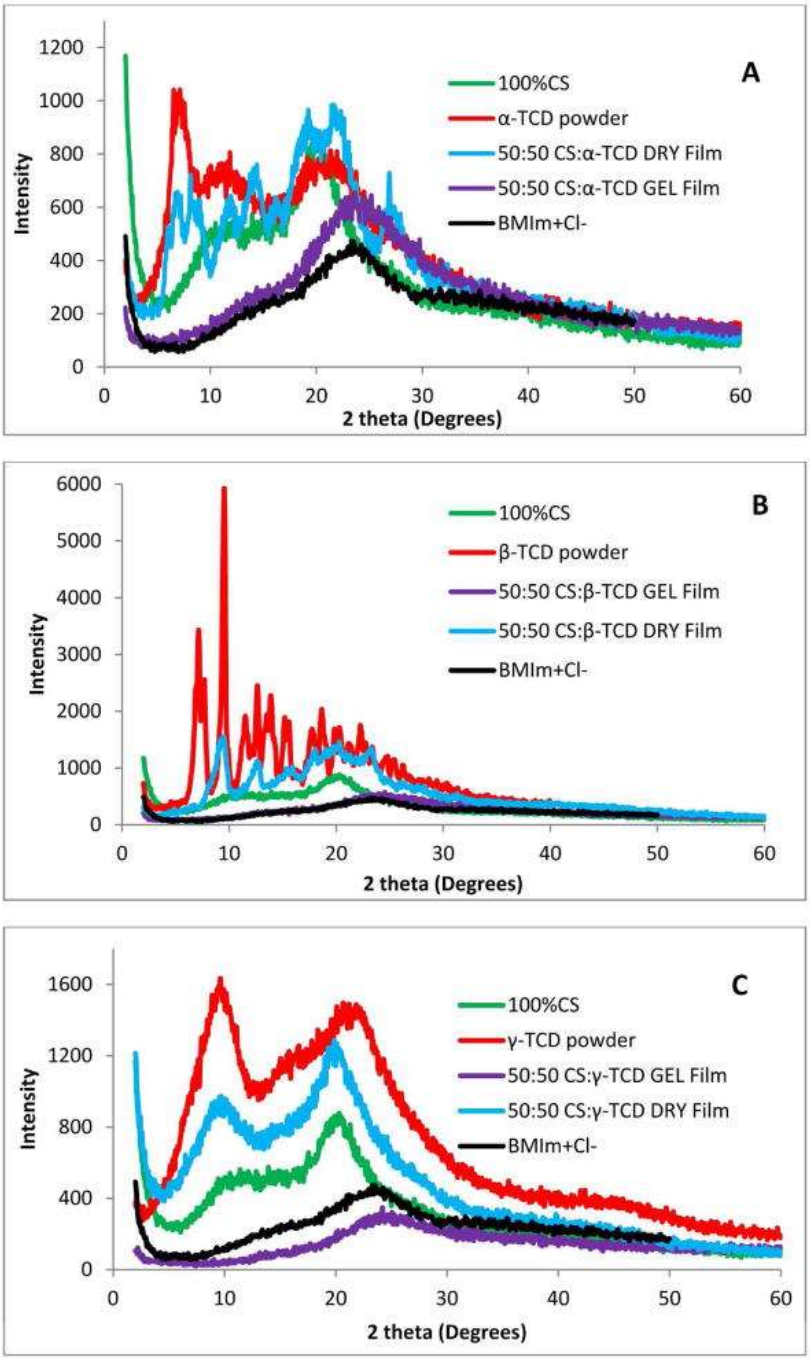

Figure 1. X-ray powder diffraction spectra of [$BMIm^+Cl^-$], CS powder, α-TCD, β-TCD and γ-TCD powder, and [CS+α-TCD] (A), [CS+β-TCD] (B) and [CS+γ-TCD] composite materials at different stages of synthesis.

Langmuir, Vol 29, No. 16 (April 23, 2013): pg. 5037-5049. DOI.

FT-IR and NIR spectroscopy was used to characterize the chemical composition of the resultant composite films. The FT-IR and NIR spectra of the α-TCD powder, 100%CS and [CS+ α-TCD] composite materials are shown in Figure 2A and 2B, respectively (those corresponding to β-TCD and γ-TCD are shown in Figure SI-2A&B and SI-3A&B of Supporting Information). As illustrated, the FT-IR spectrum of a 100% CS Dried Film displays characteristic CS bands around 3400cm^{-1} (O-H stretching vibrations), 3250 – 3350cm^{-1} (symmetric and asymmetric N-H stretching), 2850 – 2900cm^{-1} (C-H stretching), 1657cm^{-1} (C=O, amide 1), 1595 cm^{-1} (N-H deformation), 1380cm^{-1} (CH_3 symmetrical deformation), 1319cm^{-1} (C-N stretching, amide III) and 890 – 1150cm^{-1} (ether bonding).[21,35–37] For reference, FT-IR spectrum of α-TCD starting material is also shown as red curve in 2A (and those β- and γ-TCD powder are in Figure SI-1A and B, respectively). The spectrum of α-TCD powder in 2A and of β- and γ-TCD powder in SI-2A and B are very similar to one another which is as expected because these three compounds differ only in the number of glucose moieties making up the ring. The dominant absorption bands of these spectra are those due to C=O stretching vibration at ~ 1746cm^{-1}; medium and weak bands at ~ 1372cm^{-1} and 1434 cm^{-1} can be attributed to the symmetric and asymmetric deformation of CH_3 group of acetates, C-O asymmetric stretching vibration of acetates at ~ 1216cm^{-1} and the asymmetric stretching vibration of the O – CH_2 – C groups for acetates.[21,47,48] Also included as a blue curve is the FT-IR spectrum of the 50:50 CS:α-TCD composite film. In addition to bands due to CS, the composite material also exhibits, as expected, all bands which are due to the α-TCD as described above.

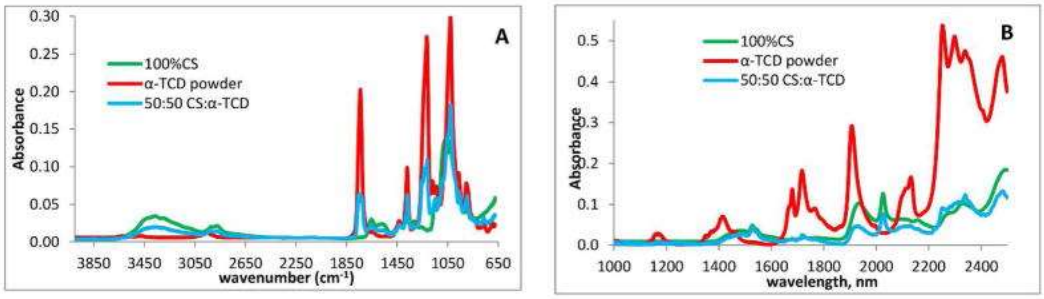

Figure 2. (A) FTIR and (B) NIR spectra of 100% CS, α-TCD and 50:50 CS: α-TCD composite material

Results from NIR measurements further confirm the successful incorporation of the TCDs into CS (Figure 2B and SI-3) and CEL

(Figure SI-4 of Supporting Information). The 100% CS film exhibits NIR absorption bands around 1492nm, 1938nm and 2104nm (Fig 2B) which can be assigned to the overtone and combination transitions of the –OH group.[21,28,46,48] In addition, CS also exhibits bands ~1548nm and 2028nm, which is due to the –NH groups.[49]

Similar to FT-IR, the NIR spectra of α-, β- and γ-TCD are also very similar. The major bands for these are around 1415nm (first overtone of methyl -CH group), 1680nm and 1720nm (first overtone of -CH group), 1908nm and 2135nm (-C=O, acetyl group).[50] As shown in figure 2B (and SI-3A and B), the NIR spectra of [CS+α-TCD], [CS+β-TCD] and [CS+γ-TCD] composite materials contain bands due to both CS and TCDs.

Similarly, FT-IR and NIR results also confirm that α-TCD, β-TCD and γ-TCD were successfully incorporated into CEL. For clarity, FT-IR and NIR spectra of only β-TCD powder, 50:50 CEL:β-TCD together with 100% CEL film are shown in Figure SI-4A and B, respectively. 100% CEL film (green curve in SI-4A) exhibits three pronounced bands at around 3400cm^{-1}, 2850 – 2900cm^{-1} and 890 – 1150cm^{-1}. These bands can be tentatively assigned to stretching vibrations of O-H, C-H and -O- group, respectively.[44] Similar to CS composite materials, FT-IR and NIR spectra of [CEL+β-TCD] composite material (as well as [CEL+α-TCD] and [CEL+γ-TCD] composites, spectra not shown) also exhibit bands due to both TCDs and CEL.

Analysis of the composite materials by SEM reveals some interesting features about the microstructure of the materials. Shown in Figure 3 are surface (images on left column) and cross section images (images on right column) of regenerated one component 100%CEL and 100%CS film (first and second row) and 50:50 [CEL+γ-TCD], [CEL+β-TCD], [CS+γ-TCD] and [CS+β-TCD] (row 3–6). As expected, both surface and cross section images clearly indicate that onecomponent CEL and CS are homogeneous. Chemically, the only difference between CS and CEL is amino in the former. However, their structures, as recorded by the SEM are substantially different. Specifically, while CS exhibits a rather smooth structure, CEL seems to arrange itself into fibrous structure with fibers having diameter of about ~0.5–1.0 micron. Interestingly, the structure of a 50:50 composite between CS and γ-TCD (images on row 5) seems to be very

Langmuir, Vol 29, No. 16 (April 23, 2013): pg. 5037-5049. DOI.

much different from that of the 50:50 [CS+β-TCD] (images on row 6). SEM images of the latter seem to indicate that it has rather smooth structure which is different from the rather fibrous structure of the 50:50 [CS+γ-TCD] composite. Similarly, the microstructure of the 50:50 [CEL+γ-TCD] (row 3) is also different from that of [CEL+β-TCD]. It is known that β-CD, being relatively small, has a rather rigid structure whereas the large γ-CD has a more flexible structure. Also γ-CD is very soluble in water (23.2g/100mL of water) whereas β-CD can hardly dissolve in water (1.85g/100mL). It is possible that because of these difference, when β-TCD forms a composite with either CS or CEL, it will adopt a microstructure which is much different from that of a composite between γ-TCD with either CEL or CS.

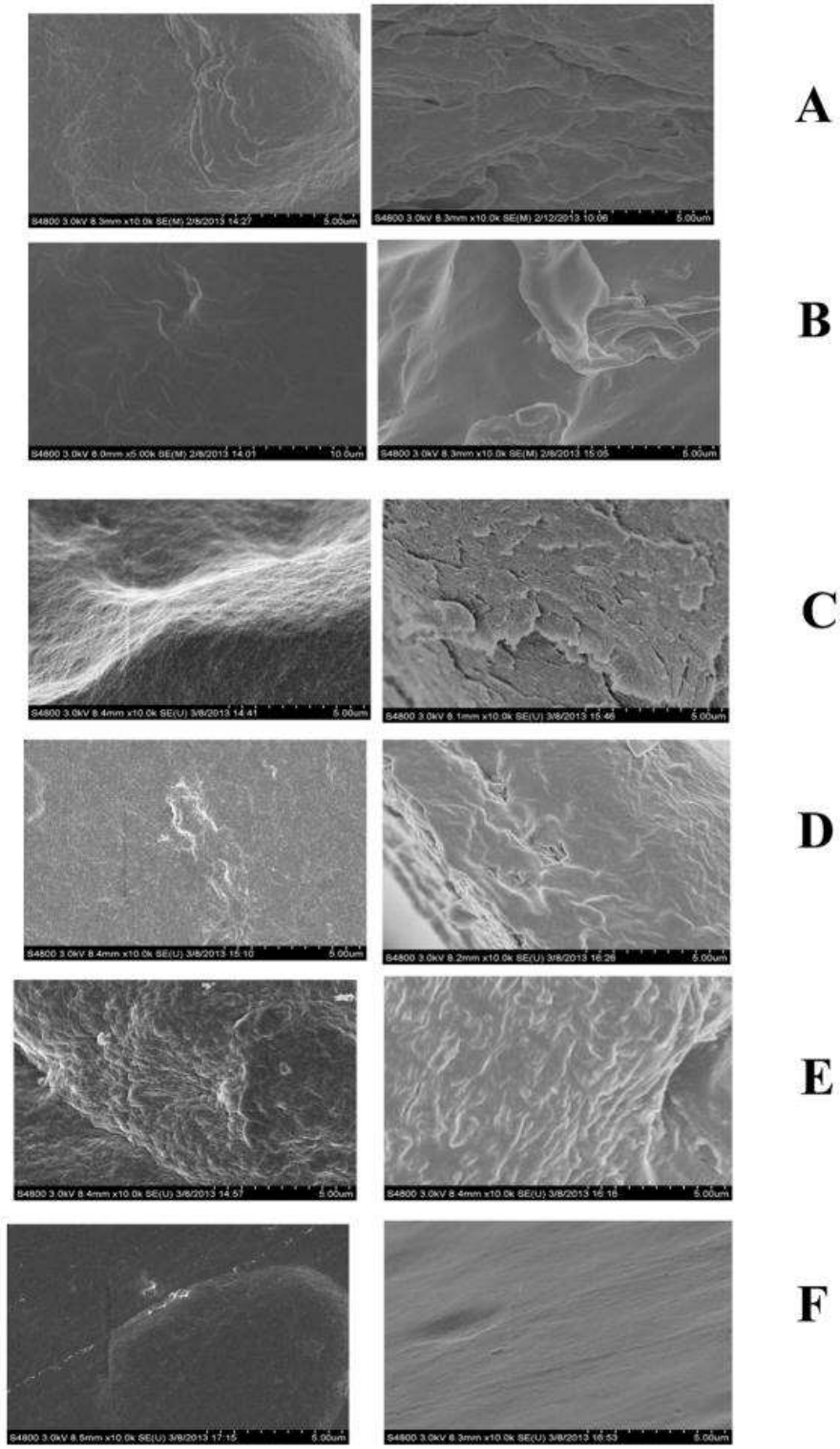

Figure 3. SEM images of surface (images on left column) and cross section (images on right column) of (A) 100%CEL, (B) 100%CS, (C) 50:50 CEL:γ-TCD, (D) 50:50 CEL"β-TCD, (E) 50:50 CS:γ-TCD and (F) 50:50 CS:β-TCD.

Langmuir, Vol 29, No. 16 (April 23, 2013): pg. 5037-5049. DOI.

As described above, mechanical and rheological strength of CDs is so poor that practically they cannot be fabricated into films for practical applications. Measurements were made to determine tensile strength of [CEL+TCDs] and [CS+TCDs] composite films with different CEL and CS concentrations in order to determine if adding CEL or CS would provide the composite material adequate mechanical strength for practical applications. Results obtained, shown in Fig 4, clearly indicate that adding either CEL or CS into the composite materials substantially increase their tensile strength. For example, up to 2X (or 6X) increase in tensile strength can be achieved by increasing concentration of CEL in [CEL+γ-TCD] composite (or CS in [CS+γTCD]) from 50% to 75%. Also, the tensile strength of the[CEL+γ-TCDs] composite is relatively higher than the corresponding [CS+γ-TCDs] composite. This is hardly surprising considering the fact that the mechanical and rheological strength of CEL is relatively higher than that of CS. It is thus, evidently clear that the [CEL+TCD] and [CS+TCD] composite materials have overcome the major hurdle currently imposed on utilization of the materials, namely they have the required mechanical strength for practical applications.

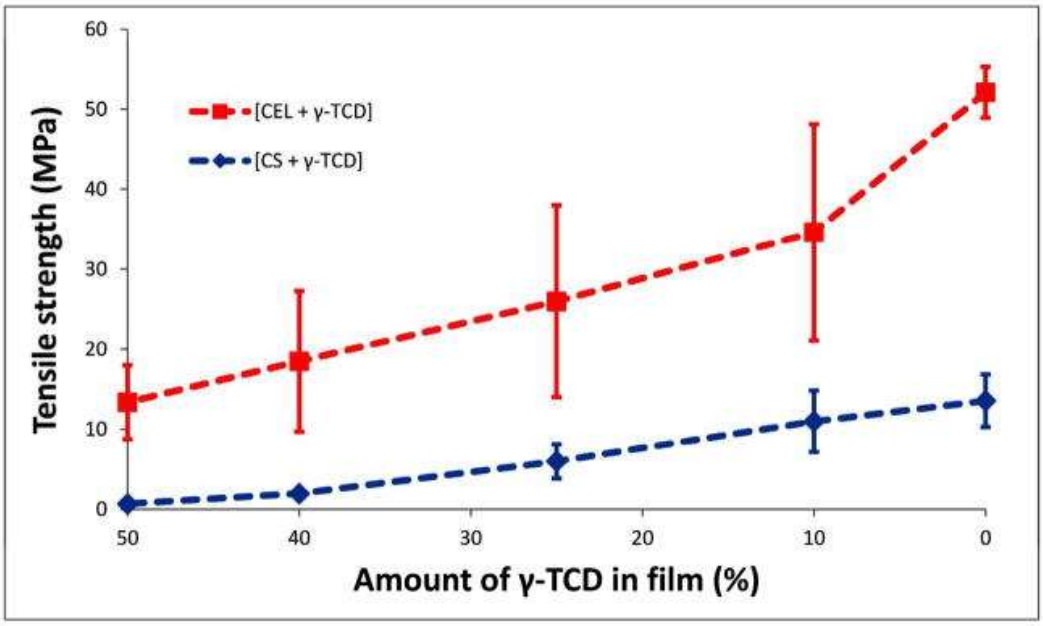

Figure 4. Plot of tensile strength as a function of γ-TCD concentration in [CEL+γTCD] composites (red curve) and [CS+γTCD] composites (blue curve).

Taken together, XRD, FT-IR, NIR and SEM results presented clearly indicate that novel all polysaccharide composite materials

containing CEL, CS and α-TCD, β-TCD and γ-TCD were successfully synthesized by use of [$BMIm^+Cl^-$], an ionic liquid, as the sole solvent. Since majority (at least 88%) of [$BMIm^+Cl^-$] used was recovered for reuse, the method recyclable. As anticipated, adding CEL (or CS) into the composites substantially increases mechanical strength of the composites. It is expected that the composites may also retain properties of CS and TCDs, namely, they would be good adsorbent for pollutants (from CS) and selectively form inclusion complexes with substrates of different sizes and shapes (from TCDs). Initial evaluation of their ability to selectively adsorb various endocrine disruptors including polychlrophenols and bisphenol A is described in following section.

3.2. Adsorption of Endocrine Disruptors (2-, 3-, and 4-chlorophenol, 3,4-dichlorophenol, 2,4,5-trichlorophenol and bisphenol A)

3.2.1. Adsorption Kinetics

Experiments were designed to determine: (1) if CEL, CS, [CEL+TCD] and [CS+TCD] composite materials can adsorb chlorophenols and bisphenol A; (2) if they can, rate constants, adsorbed amounts at equilibrium (q_e) and mechanism of adsorption processes; (3) composite material which gives highest adsorption; and (4) if TCDs can provide any selectivity on adsorption of analytes with different sizes and shapes. These were accomplished by initially fitting kinetic data to both pseudo-first order and pseudo-second order models. Appropriate reaction order for the adsorption processes was determined based on the correlation coefficients (R^2) and the Model Selection Criteria (MSC) values. Rate constants and q_e values were then obtained from the kinetic resutls.[51, 52] Subsequent fitting of data to intra-particle diffusion model together with results of adsorption isotherms measurements yielded additional insight into adsorption process.

The pseudo first order and pseudo second order kinetic models were used to obtain the rate constants and equilibrium adsorption capacity of 100%CEL, 100%CS, 50:50 CS:β-TCD and 50:50 CEL:β-TCD composite materials for different analytes including chlorophenols

Langmuir, Vol 29, No. 16 (April 23, 2013): pg. 5037-5049. DOI.

and bisphenol A. Results obtained by pseudo-1st order and pseudo-2nd order fitting of adsorption of all analytes by 100%CEL, 100%CS, 50:50 CS:β-TCD and 50:50 CEL:β-TCD are listed in Table SI-1-4 (of Supporting Information). In all cases, the R^2 and the MSC values are higher for the pseudo-2nd order kinetic model than those corresponding for the pseudo first order kinetic model. In addition, the theoretical and experimental equilibrium adsorption capacities, q_e, obtained for the pseudo-1st order kinetic model varied widely for the different analytes. The results seem to suggest that the adsorption of various chlorophenols and BPA onto 100%CEL, 100%CS, 50:50 CS:β-TCD and 50:50 CEL:β-TCD composite materials is best described by the pseudo-2nd order kinetic model. Good correlation of the system provided by the pseudo-2nd order kinetic model suggest that chemical sorption involving valence forces through sharing or exchange of electrons between adsorbent and analyte might be significant.[52]

Additional information on mechanism of adsorption can be gained by analyzing data using Intra-particle diffusion model as described in the Supporting Information. Shown in figure 5 are representative intra-particle pore diffusion plots (q_t versus $t^{1/2}$) for three of the analytes studied, 3,4-Di-Cl-Ph, 2,4,5-Tri-Cl-Ph and BPA adsorbed on 50:50 CEL: β-TCD and 50:50 CS: β-TCD composites. As illustrated, plots of q_t versus $t^{1/2}$ are not linear but rather non-linear which can be fitted to two linear segments for all analytes on both composites with the exception that data for 2,4,5-Tri-Cl-Ph on 50:50 CS: β-TCD may possibly be fitted to a linear regression with R^2=0.9819. According to this model, the 1st sharper linear region can be assigned to the instantaneous adsorption or external surface adsorption, while the second region may be due to gradual adsorption stage where intra-particle diffusion is the rate limiting.[51, 53] These results seem to imply that the intra-particle diffusion is not the sole rate controlling step but other mechanisms may also contribute to the adsorption process.

Langmuir, Vol 29, No. 16 (April 23, 2013): pg. 5037-5049. DOI.

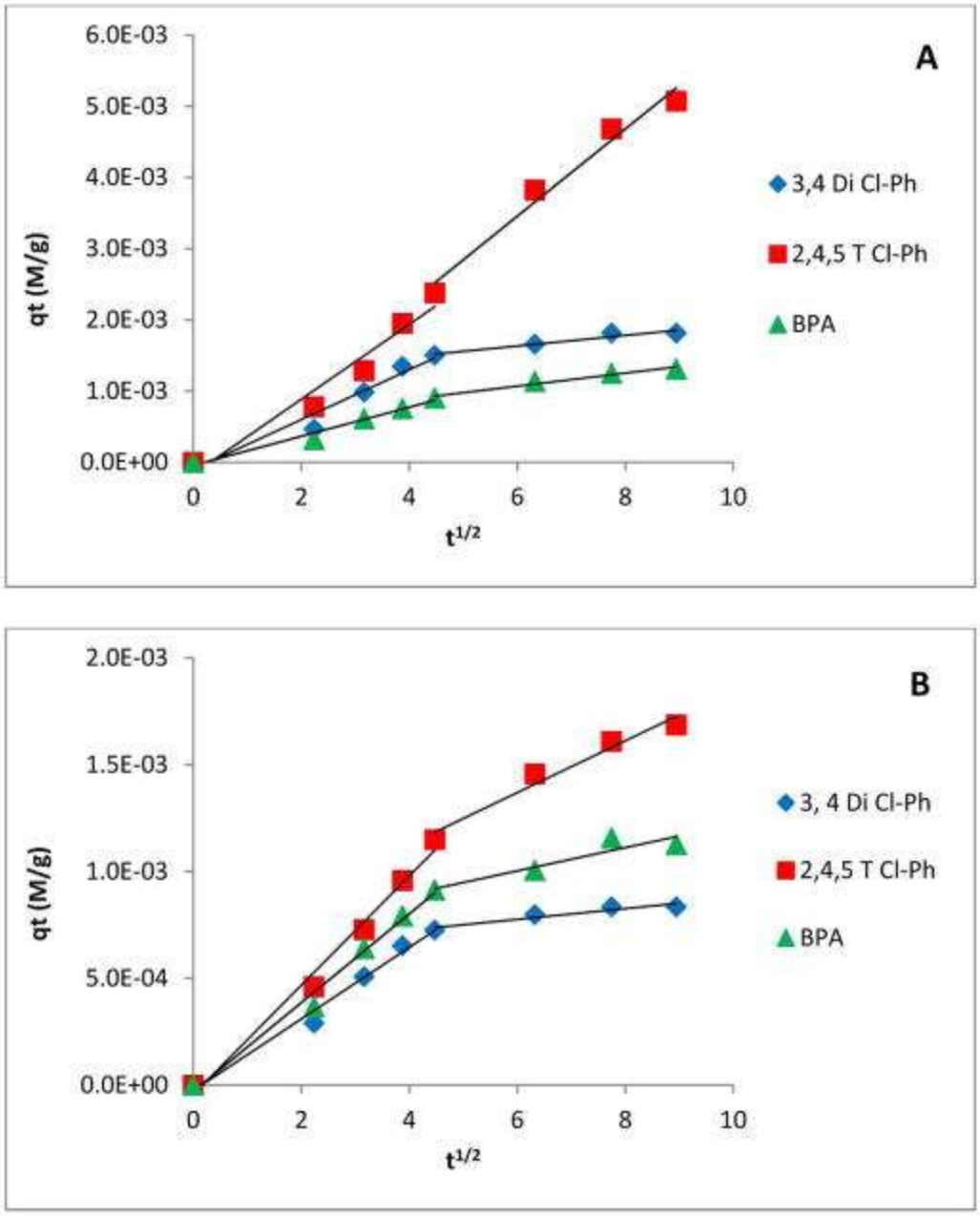

Figure 5. Intra-particle pore diffusion model plots for A) 50:50 CS:β-TCD and B) 50:50 CEL:β-TCD

Results obtained from the pseudo-2nd order kinetics in terms of equilibrium sorption capacity (q_e) and rate constant (k_2) were then used to evaluate sorption performance of the composite materials. Table 1 lists q_e and k_2 values for 5 different chlorophenols and BPA on 100%CEL, 50:50 CEL:β-TCD, 100%CS and 50:50 CS:β-TCD, respectively. For clarity of presentation and discussion, data from the

tables were used to construct three plots for three pairs of composites: 100%CEL and 100%CS (Fig 6A), 100%CEL and 50:50 CEL:β-TCD (Fig 6B) and 100%CS and 50:50 CS:β-TCD (Fig 6C). Figure 6D plots results obtained for all analytes by all composite materials.

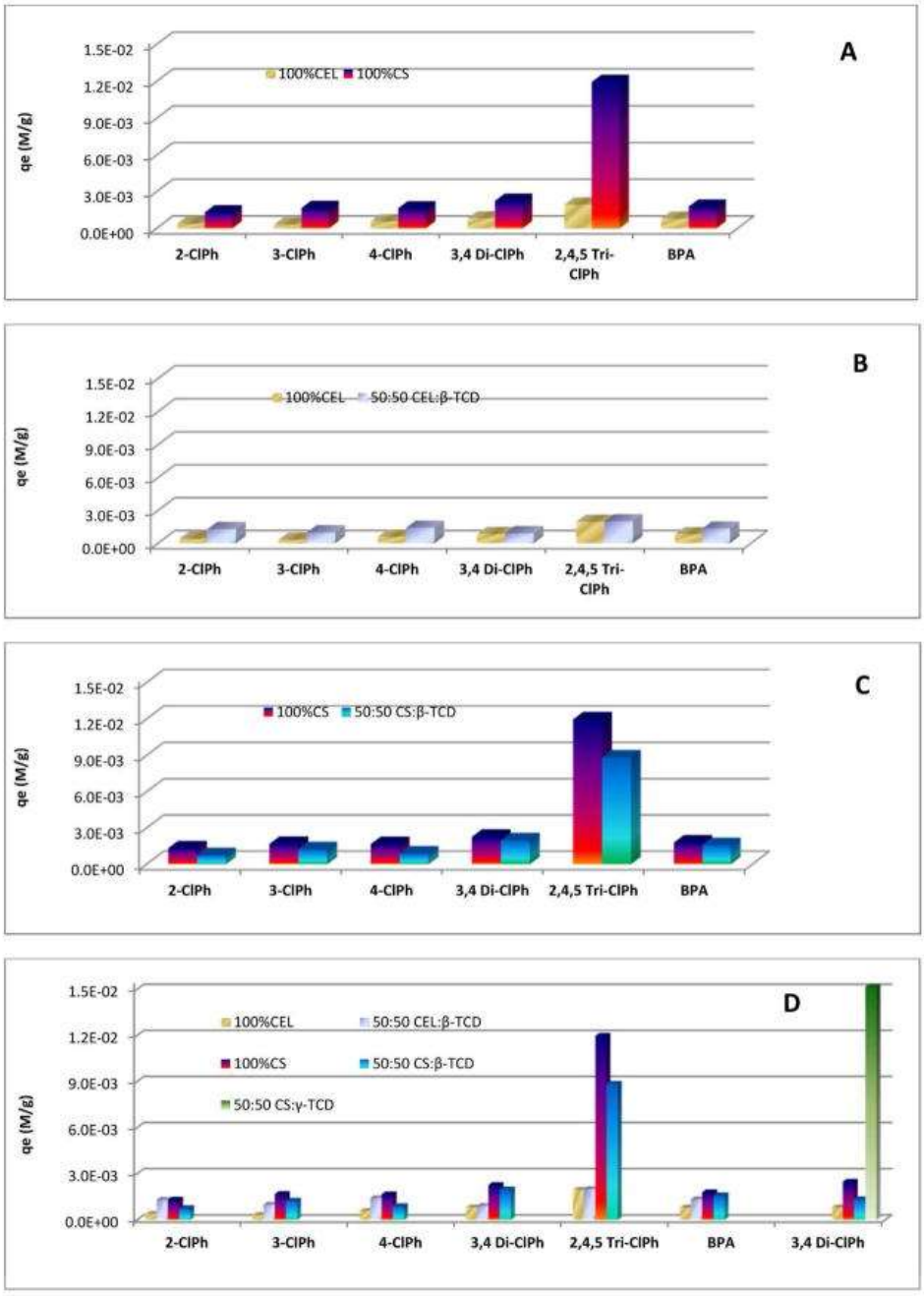

Figure 6. Plot of equilibrium sorption capacity (q_e) of all analytes by (A) 100%CEL and 100%CS; (B) 100%CEL and 50:50 CEL:β-TCD; (C) 100%CS and 50:50 CEL:β-TCD; and (D) all four composites.

Table 1. Comparison of pseudo second order kinetic parameters for 100% CEL, 100% CS, 50:50 CEL:β-TCD and 50:50 CS:β-TCD composite material.

Table 1. Comparison of Pseudo-Second-Order Kinetic Parameters for 100% CEL, 100% CS, 50:50 CEL/β-TCD, and 50:50 CS/β-TCD Composite Materials

	100% CEL				100% CS				50:50 CEL/β-TCD				50:50 CS/β-TCD			
analyte	q_e (M/g)	k_2 (M^{-1} min^{-1})	R^2	MSC	q_e (M/g)	k_2 (M^{-1} min^{-1})	R^2	MSC	q_e (M/g)	k_2 (M^{-1} min^{-1})	R^2	MSC	q_e (M/g)	k_2 (M^{-1} min^{-1})	R^2	MSC
2-ClPh	3.93×10^{-4}	702.3	0.9871	3.95	1.32×10^{-3}	385.9	0.9998	8.02	1.30×10^{-4}	100.2	0.9975	5.57	7.59×10^{-4}	288.4	0.9947	5.32
3-ClPh	3.20×10^{-4}	393.6	0.9832	5.72	1.68×10^{-3}	133.5	0.9960	5.21	8.87×10^{-4}	77.9	0.9984	5.33	1.25×10^{-3}	128.6	0.9934	4.71
4-ClPh	5.81×10^{-4}	2054.2	0.9999	9.13	1.66×10^{-3}	214.8	0.9998	7.52	1.41×10^{-4}	58.8	0.9983	8.93	8.99×10^{-4}	313.1	0.9957	5.11
3,4 Di-ClPh	8.19×10^{-4}	315.6	0.9996	7.47	2.27×10^{-3}	169.8	0.9999	8.72	9.12×10^{-4}	160.6	0.9992	6.84	1.99×10^{-3}	57.1	0.9978	5.77
2,4,5 Tri-ClPh	1.95×10^{-3}	21.6	0.9967	5.52	1.20×10^{-2}	2.1	0.9991	6.60	2.00×10^{-3}	33.2	0.9995	7.26	8.84×10^{-3}	2.1	0.9996	7.01
BPA	8.05×10^{-4}	70.9	0.9911	4.59	1.80×10^{-3}	166.3	0.9995	7.24	1.34×10^{-3}	65.3	0.9987	6.28	1.59×10^{-3}	37.0	0.9994	7.11

It is evident from Fig 6A that, for all analytes, equilibrium sorption capacities for 100% CS material are much higher than those corresponding for 100%CEL material; e.g., for 2,4,5-Tri-Cl-Ph, the 100%CS material exhibits up to 6X more equilibrium sorption capacity than the 100%CEL material. Even for BPA, where the difference between CEL and CS materials are smallest, the CS material still has a q_e value twice as much as that of the CEL material. This is as expected, because CEL is known to be inert whereas CS is reported to be an effective adsorbent for various pollutants.

Additional experiments were then performed to further confirm these results. Specifically, six different [CEL+CS] composite materials with different CEL and CS compositions were synthesized, and their adsorption of 2,4,5 trichlorophenol was measured. Results obtained, in terms if q_e and k_2 values, plotted as a function of CS concentration in the composites are shown in Figure 7A. It is evident that adding CS into CEL resulted in improved uptake of 2,4,5 trichlorophenol. For example, q_e value was increased by 5 folds when 50% of CS was added to CEL, and the equilibrium sorption capacity seems to be proportional to concentration of CS in the composite. These results clearly indicate that CS is responsible for adsorption of the endocrine disruptors, and that sorption capacity of a composite toward endocrine disruptors can be set at any value by judiciously adjusting concentration of CS in the composite.

Langmuir, Vol 29, No. 16 (April 23, 2013): pg. 5037-5049. DOI.

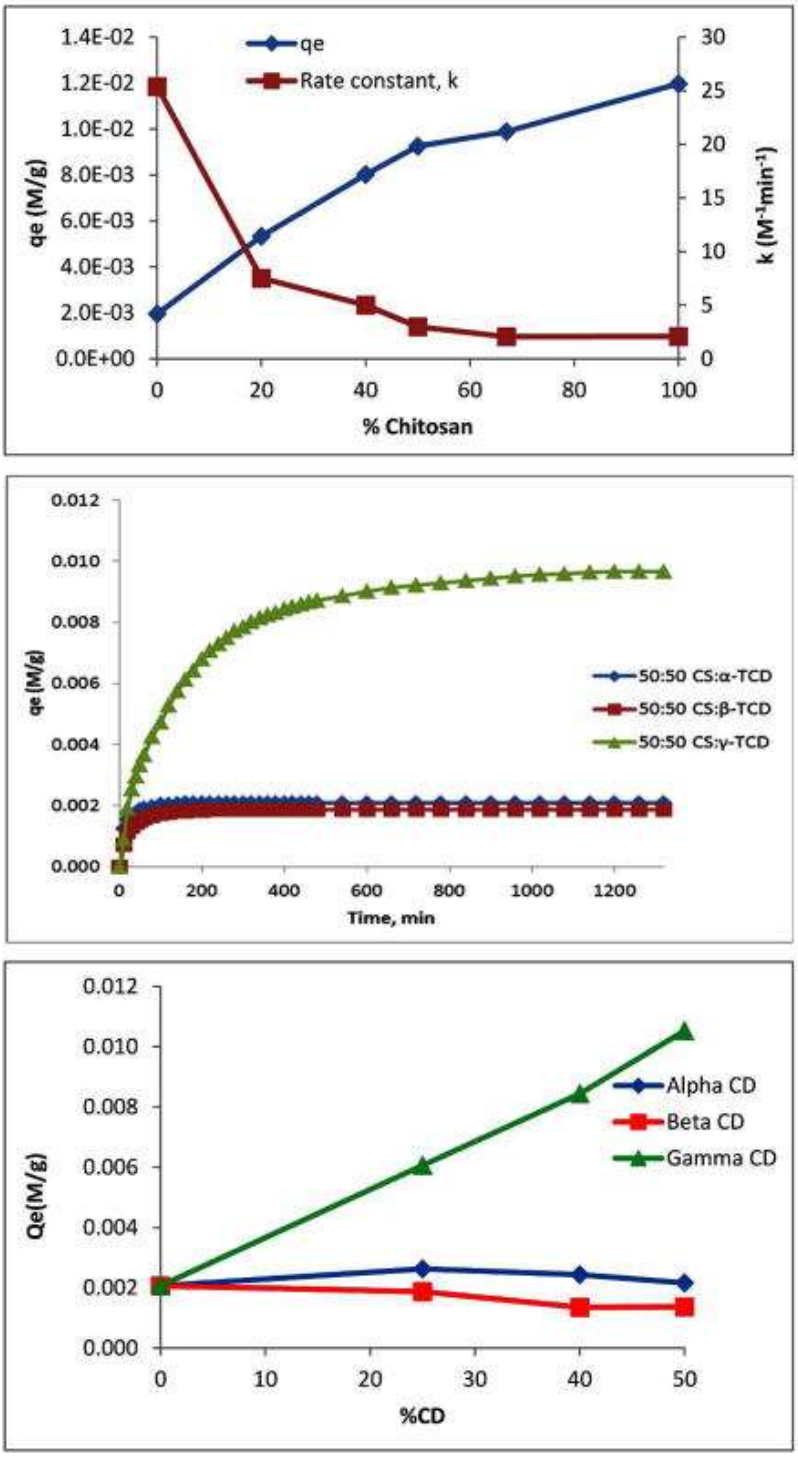

Figure 7. Plot of (A) q_e and k for adsorption of 2,4,5-tri-chlorophenol as a function of CS concentration in [CEL+CS] composite materials; (B) Sorption profiles of 50:50 CS:α-TCD, 50:50 CS:β-TCD and 50:50 γ-TCD CS composites for 3,4 di Cl-Ph; and (C) Equilibrium sorption capacity for 3,4-dichlorophenol by CS+TCD composite materials as a function of α-TCD, β-TCD and γ-TCD concentration in the composites.

Langmuir, Vol 29, No. 16 (April 23, 2013): pg. 5037-5049. DOI.

When added to CEL, β-TCD seems to exert much different effect on equilibrium sorption capacity than that of CS. As illustrated in Fig 6B, substantial enhancement in q_e values was observed when 50% of β-TCD was added to CEL, but the enhancement was not observed for all analyte (as were seen for CS) but only for four analytes; i.e., about 3-fold enhancement for, 2- and 3-chlorophenol and about 2X for 4-chlorophenol and bisphenol-A. Within experimental error, no observable enhancement was observed for 3,4-dichlorophenol and 2,4,5-trichlorophenol when 50% of β-TCD was added to CEL. A variety of reasons might account for lack of enhancement for 3,4-dichloro and 2,4,5-trichlorophenol but the most likely one is probably due to the bulky dichloro- and trichloro groups on these compounds which sterically hinders their ability to form inclusion complexes with β-TCD.

To further investigate difference effect of CS and β-TCD on adsorption process, adsorption results by 100%CS and 50:50 CS: β-TCD for all analytes were plotted in Figure 6C. Compared to β-TCD, CS has relatively higher q_e values for all analytes including 3,4-dichloro- and 2,4,5-trichlorophenol. The latter two compounds, as described above, may not be able to be included in the cavity of β-TCD because of their bulky groups. The results seem to indicate that CS may adsorb the analytes by mechanism which is different from that of the β-TCD, namely surface adsorption appears to be the main and only adsorption mechanism for CS whereas the inclusion complex formation seems to be the main adsorption process for β-TCD with surface adsorption being the secondary mechanism. It is expected that while efficiency for surface adsorption by CS is relatively higher than that of inclusion complex formation, it may not provide any selectivity due to size and shape of host as well as guest compounds. To investigate this possibility, adsorption of 3,4-dichlorophenol by 50:50 CS:γ-TCD as well as by 100%CEL, 100%CS, 50:50 CEL: β-TCD and 50:50 CS: β-TCD were measured and results are presented as the last group on the far right of figure 6D. As expected, results obtained further confirm the proposed mechanism. Specifically, 3,4-dichlorophenol, as described in previous section, because of its bulky dichloro group, cannot form inclusion complexes with β-TCD. Therefore, it was adsorbed by CS as well as by β-TCD mainly through surface adsorption. Conversely, γ-TCD with its cavity about 58% larger than that of β-TCD, can well accommodate 3,4-dichlorophenol to its cavity through inclusion complex formation which leads to substantial enhancement in

adsorption capacity for 50:50 CS:γ-TCD as compared to other composites.

Additional evidence to confirm inclusion complex formation and size selectivity provided by TCD is shown in Figure 7B which plots the sorption profiles for 3,4-dichlorophenol by 50:50 CS:α-TCD, 50:50 CS:β-TCD and 50:50 CS:γ-TCD. As expected, because the cavities of α-TCD and β-TCD are too small to accommodate 3,4-dichlorophenol, the latter can only be adsorbed onto 50:50 CS:α-TCD and 50:50 CS:β-TCD by surface adsorption which led to low and similar adsorption curve for both composite materials. Conversely, 50:50 CS:γ-TCD with its larger γ-TCD, can readily form inclusion complexes with 3,4-dichlorophenol, and as a consequence, can adsorb much more analyte, i.e. substantially higher sorption profile.

Plot of equilibrium sorption capacity (q_e) for 3,4-dichlorophenol by CS+α-TCD, CS+β-TCD and CS+γ-TCD as a function of α-, β- and γ-TCD concentration in the composites are shown in Figure 7C. Again, since 50:50 CS:α-TCD and 50:50 CS:β-TCD cannot form inclusion complex with 3,4-dichlorophenol, their q_e values remain the same regardless of the concentration of α- and β-TCD in the composite materials. Not only that q_e profile of CS+γ-TCD material is different and much higher than those for CS+α-TCD and CS+β-TCD but also q_e value is proportional to the concentration of γ-TCD in the composite material. For example, adding 50% γ-TCD to CS material led up to 5 folds increase in q_e value. This is probably due to the fact that because γ-TCD can readily form inclusion complexes with 3,4 dichlorophenol, increasing concentration of γ-TCD in the [CS+γ-TCD] material resulted in higher concentration of inclusion complexes, and hence higher q_e value.

3.2.2. Adsorption isotherms

To gain insight into adsorption process, investigation was then carried out to determine adsorption isotherm for adsorption of 3,4-dichlorophenol by 100%CS and 50:50 CS: γ-TCD. These two composites were selected because kinetic results presented above indicate that they adsorb 3,4-dichlorophenol by two distinct different mechanisms: surface adsorption and inclusion complex formation. Experimental results were fitted to three different models, Langmuir

isotherm[54], Freundlich isotherm[55] and the Dubinin-Radushkevich (D-R) isotherm.[56, 57] (See Supporting Information for detailed description of these three models). Fitting of experimental values to these three models is shown in Figure 8. The parameters obtained from fits to these models are listed in table 2. As listed, experimental values fit relatively well to theoretical models. For example, R^2 values for fit of 100%CS and 50:50 CS:γ-TCD composites to the Langmuir, the Freundlich and the D-R model were found to be 0.977 and 0.984, 0.970 and 0.949, and 0.972 and 0.912, respectively. Relatively good agreement was also found for the saturation adsorption capacity q_{max} values obtained with the Langmuir model and the D-R model: 137.6 mg/g and 102.6 mg/g by 50:50 CS:γ-TCD, and 63.2 mg/g and 26.7 mg/g by 100% CS. The good fit between the Langmuir isotherm model and the experimental data suggests that the sorption is monolayer; sorption of each molecule has equal activation energy and that the analyte-analyte interaction is negligible.[58]

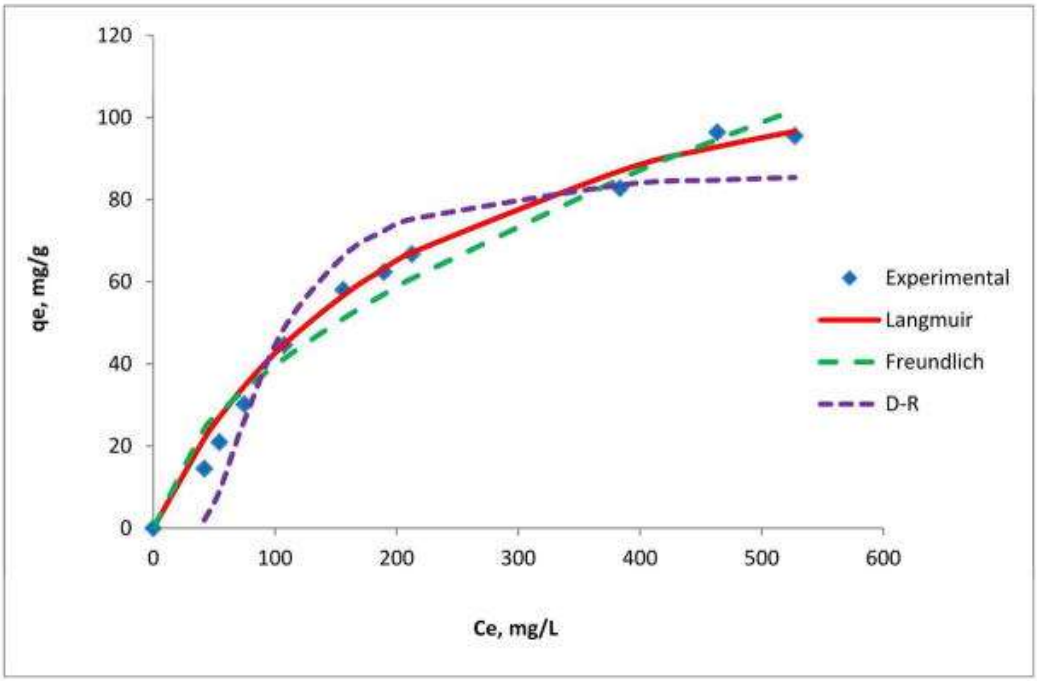

Figure 8. Fitting of experimental values to Langmuir, Freundlich and Dubinin-Radushkevich isotherm model for the adsorption of 3,4 di Cl-Ph onto 50:50 CS:γ-TCD composite material.

Langmuir, Vol 29, No. 16 (April 23, 2013): pg. 5037-5049. DOI.

Table 2. Adsorption isotherm parameters for the adsorption of 3, 4 dichlorophenol onto 100%CS and 50:50 CS:γ-TCD Composite Materials

	3, 4-dichlorophenol									
	Langmuir Isotherm parameters			Freundlich isotherm parameters			D-R isotherm parameters			
	q_{max}(mg/g)	K_L(L/mg)	R^2	n	K_F(mg/g)(L/mg)1/n	R^2	q_{max}(mg/g)	β(mmol^{2}J^{-2})	E (kJ/mol)	R^2
100 % CS	63.2	0.0004	0.977	1.0	0.015185	0.970	26.7	0.0805	2.5	0.972
50:50 CS:γ-TCD	137.6	0.0045	0.984	1.4	1.34975	0.949	102.6	0.0026	13.9	0.912

Additional information on the adsorption process can be obtained from the Freundlich isotherm model, particularly from the constant n in Eq SI-8 (of Supporting Information) because it is known to be a measure of the favorability of the sorption process.[58] Because n was found to be 1.0 and 1.4 for 100%CS and 50:50 CS:γ-TCD, respectively, the adsorption of 3,4 dichlorophenol by the latter seems to be more favorable than that of the former.

From the fitting to Dubinin–Radushkevich isotherm model, the mean free energy E values of the sorption process per mole of 3,4 di Cl-Ph were found to be 2.5 KJ/mol and 13.9 KJ/mol for 100%CS and 50:50 CS:γ-TCD, respectively. According to this theory (see Supporting Information for detailed information), the sorption of 3,4 di Cl-Ph onto 50:50 CS:γ-TCD composite film is chemisorption and is much stronger than onto 100%CS which is more by physisorpiton. This finding is as expected because as described above, 50:50 CS:γ-TCD composite material can readily form inclusion complexes with 3,4-dichlorophenol, and adsorption by inclusion complex formation is relatively stronger and is chemisorb by nature compared to 100%CS which can adsorb the analyte only by surface adsorption.

Taken together, adsorption isotherm results fully support kinetic results. Specifically, both results clearly indicate that 50:50 CS:γ-TCD with its ability to form inclusion complexes with 3,4-dichlorophenol, can strongly and effectively adsorb much more analyte compared to 100% CS which can only adsorb by surface adsorption which is relatively weaker and less effective.

Langmuir, Vol 29, No. 16 (April 23, 2013): pg. 5037-5049. DOI.

4. Conclusions

In summary, we have successfully developed a novel, simple and one step method to synthesize novel, high performance supramolecular polysaccharide composite materials from CEL, CS and α-, β- and γ-TCD. [$BMIm^+Cl^-$], an ionic liquid (IL), was used as a sole solvent for dissolution and preparation of the composites. Since majority (more than 88%) of [$BMIm^+Cl^-$] used was recovered for reuse, the method is recyclable. The [CEL/CS+TCDs] composites obtained retain properties of their components, namely superior mechanical strength (from CEL), excellent adsorption capability for pollutants (from CS) and ability to selectively form inclusion complexes with substrates with appropriate sizes and shapes (from γ-TCDs). Specifically, both CS- and TCD-based composite materials can effectively adsorb pollutants such as endocrine disruptors, e.g., chlorophenols and bisphenol A. While CS-based composites can effectively adsorb the pollutants, its adsorption is independent on the size and structure of the analytes. Conversely, the adsorption by TCD-based composites exhibits strong dependency on size and structure of the analytes. For example, while all three TCD-based composites (i.e., α-, β- and γ-TCD) can effectively adsorb 2-, 3- and 4-chlorophenol, only γ-TCD-based composite can adsorb analytes with bulky groups including 3,4-dichloro- and 2,4,5-trichlorophenol. Furthermore, equilibrium sorption capacities for the analytes with bulky groups by γ-TCD-based composite are much higher than those by CS-based composites. These results together with results from adsorption kinetics and adsorption isotherm clearly indicate that γ-TCD-based composite with its relatively larger cavity size can readily form inclusion complexes with analytes with bulky groups, and through inclusion complex formation, it can strongly adsorb much more analytes and with size/structure selective compared to CS-based composites which can adsorb the analyte only by surface adsorption. For example, up to 138 mg of 3,4-dichlorophenol can be adsorbed by 1g of 50:50 CS:γ-TCD composite material compared to only 63mg of 3,4-dichlorophenol per 1g of 100%CS material. Preliminary results presented in this study are very encouraging and clearly indicate that higher adsorption efficiency can be obtained by judiciously modifying experimental conditions (e.g., replacing film of composite materials with microparticles to increase surface area). Furthermore, since all

composite materials used in this study (CEL, CS, CEL+TCD, CS+TCD) are chiral because of their glucose and glucosamine units in CEL, CS and TCD, it is expected that they may exhibit some stereospecificity in the adsorption of chiral analytes. These possibilities are the subject of our current intense study.

We developed a simple, green and totally recyclable method to prepare supramolecular polysaccharide composites from cellulose (CEL), chitosan (CS) and cyclodextrins (α-, β- and γ-CD). The composites retain unique properties of each component including superior mechanical properties (from CEL), excellent adsorbent for pollutants and toxins (from CS) and ability to selectively form inclusion complexes with substrates with appropriate size and shape (from CDs).

Acknowledgments

Research reported in this publication was supported by the National Institute of General Medical Sciences of the National Institutes of Health under Award number R15GM099033.

Footnotes

Supporting Information. Information on analysis of Kinetic Data and equilibrium sorption isotherms can be found in the Supporting Information. This material is available free of charge via the Internet at http://pubs.acs.org

References

[1] Katsuhiko A, Kunitake T. Supramolecular Chemistry-Fundamentals and Applications. Springer; Berlin, Heidelberg: 2006.

[2] Rebek J., Jr Introduction to the molecular recognition and self-assembly special feature. Proc Nat Acad Sci. 2009;106:10423–10424.

[3] Rebek J., Jr Molecular Behavior in Small Spaces. Acct Chem Res. 2009;42:1660–1668.

[4] Hinze WL, Armstrong DW. Organized surfactant assemblies in separation science. ACS Symposium Ser. 1987;342:2–82.

[5] Fakayode SO, Brady PN, Pollard DA, Mohammed AK, Warner IM. Multicomponent analyses of chiral samples by use of regression analysis of UV-visible spectra of cyclodextrin guest-host complexes. Anal Bioanal Chem. 2009;394:1645–1653.

[6] Fakayode SO, Lowry M, Fletcher KA, Huang X, Powe AM, Warner IM. Cyclodextrins host- guest chemistry in analytical and environmental chemistry. Cur Anal Chem. 2007;3:171–181.

[7] Kitaoka M, Hayashi K. Adsorption of bisphenol A by cross-linked β-cyclodextrin polymer. J Incl Phe Macro Chem. 2002;44:429–431.

[8] Nishiki M, Tojima T, Nishi N, Sakairi N. β-Cyclodextrin-linked chitosan beads: preparation and application to removal of bisphenol A from water. Carbohydrate Let. 2000;4:61–67.

[9] Augustine AV, Hudson SM, Cuculo JA. Cellulose Sources and Exploitation. Ellis Horwood; New York: 1990.

[10] Dawsey TR. Cellulosic Polymers, Blends and Composites. Carl Hanser Verlag; New York: 1994.

[11] Masanori Y, Shinya T. DNA–cyclodextrin–inorganic hybrid material for absorbent of various harmful compounds. Mat Chem Phys. 2011;126:278–283.

[12] Murai S, Kinoshita K, Ishii S, Aoki N, Hattori K. Removal of phenolic compounds from aqueous solution by β-cyclodextrin polymer. Trans Mat Res Soc Jap. 2006;31:977–980.

[13] Bordenave N, Grelier S, Coma V. Hydrophobization and antimicrobial activity of chitosan and paper-based packaging material. Biomacromolecules. 2010;11:88–96.

[14] Rabea EI, Badawy MET, Stevens CV, Smagghe G, Steurbaut W. Chitosan as antimicrobial agent: Applications and mode of action. Biomacromolecules. 2003;4:1457–1465.

[15] Burkatovskaya M, Tegos GP, Swietlik E, Demidova TN, Castano AP, Hamblin MR. Use of chitosan bandage to prevent fatal infections developing from highly contaminated wounds in mice. Biomaterials. 2006;27:4157–4164.

[16] Rossi S, Sandri G, Ferrari F, Benferonic MC, Caramella C. Buccal delivery of acyclovir from films based on chitosan and polyacrylic acid. Pharm Dev Tech. 2003;8:199–208.

[17] Jain D, Banerjee R. Comparison of ciprofloxacin hydrochloride-loaded protein, lipid, and chitosan nanoparticles for drug delivery. J Biomed Mat Res B Appl Biomater. 2008;86:105–112.

[18] Ngah WSWAN, Isa IM. Comparison study of copper ion adsorption on chitosan, Dowex A-1: and Zerolit 225. J Appl Pol Sci. 1998;67:1067–1070.

[19] Cai J, Liu Y, Zhang L. Dilute solution properties of cellulose in LiOH/urea aqueous system. J Pol Sci B Pol Phys. 2006;44:3093– 3101.

[20] Fink HP, Weigel P, Purz HJ, Ganster J. Structure formation of regenerated cellulose materials from NMMO- solutions. Progress Pol Sci. 2001;26:1473–1524.

[21] Tran CD, Duri S, Harkins AL. Recyclable Synthesis, Characterization, and Antimicrobial Activity of Chitosan-based Polysaccharide Composite Materials. J Biomed Materials Res A. 2013;00A:000–000.

[22] Tran CD, Lacerda SHP. Determination of Binding Constants of Cyclodextrins in Room Temperature Ionic Liquids by Near-Infrared Spectrometry. Anal Chem. 2002;74:5337– 5341.

[23] Han X, Armstrong DW. Ionic Liquids in Separations. Acc Chem Res. 2007;40:1079–1086.

[24] Tran CD. Ionic Liquids Applications: Pharmaceutical, Therapeutics and Biotechnology. ACS Symposium Series. 2010;1038:35–54.

[25] Welton T. Room-Temperature Ionic Liquids. Solvents for Synthesis and Catalysis. Chem Rev. 1999;99:2071–2083.

[26] Wasserscheid P, Welton T. Ionic Liquids in Synthesis. Wiley-VCH; Weinheim, Germany: 2003.

[27] Baptista MS, Tran CD, Gao GH. Near Infrared Detection of Flow Injection Analysis by Acousto-Optic Tunable Filter Based Spectrophotometry. Anal Chem. 1996;68:971–976.

[28] Duri S, Majoni S, Hossenlopp JM, Tran CD. Determination of Chemical Homogeneity of Fire Retardant Polymeric Nanocomposite Materials by Near-infrared Multispectral Imaging Microscopy. Anal Lett. 2010;43:1780–1789.

[29] Liebert TF, Heinze TJ, Edgar KJ. Cellulose solvents: for analysis, shaping and chemical modification. ACS symposium series. 2010;1033:299–317.

[30] Baxter A, Dillon M, Taylor K, Roberts G. Improved method for I.R. determination of the degree of acetylation of chitosan. Int J Biol Macromol. 1992;14:166– 169.

[31] Domzy J, Roberts G. Evaluation of infrared spectroscopic techniques for analyzing chitosan. Makromol Chem. 1985;186:1671– 1677.

[32] Berth G, Dautzenberg H. The degree of acetylation of chitosans and its effect on the chain conformation in aqueous solution. Carbohydrate Polymers. 2002;47:39– 51.

[33] Fereira MC, Marvao MR, Duarte ML, Nunes T. Optimization of the measuring of chitin/chitosan degree of acetylation by FT-IR spectroscopy. Chitin World, [Proceedings from the International Conference on Chitin and Chitosan], 6th, Gdynia, Pol.; 1994. pp. 480–488.

[34] Fereira MC, Marvao MR, Duarte ML, Nunes T, Feio G. Chitosan degree of acetylation: comparison of two spectroscopic methods (^{13}C CP/MAS NMR and dispersive IR). Chitin World, [Proceedings from the International Conference on Chitin and Chitosan], 6th, Gdynia, Pol; 1994. pp. 476–479.

[35] Hirai A, Odani H, Nakajima A. Determination of degree of deacetylation of chitosan by ^{1}H NMR spectroscopy. Polymer Bulletin. 1991;26:87– 94.

[36] Santiago de Alvarenga E. Characterization and properties of chitosan. Biotechnology of biopolymers. 2011:91–108.
[37] Percot A, Viton C, Domand A. Characterization of shrimp shell deproteinization. Biomacromolecules. 2003;4:1380– 1385.
[38] Li B, Zhang J, Dai F, Xia W. Purification of chitosan by using sol-gel immobilized pepsin deproteinization. Carbohydrate Polymers. 2012;88:206– 212.
[39] Xu A, Wang J, Wang H. Effect of anionic structure and lithium salts addition on the dissolution of cellulose in 1-butyl-3-mrthylimidazolium-based ionic liquid solvent systems. Green Chemistry. 2010;12:268– 275.
[40] Xiao W, Chen Q, Wu Y, Wu T, Dai L. Dissolution and blending of chitosan using 1,3-dimethylimidazolium chloride and 1-H-3-methylimidazolium chloride binary ionic liquid solvent. Carbohydrate Polymers. 2011;83:233– 238.
[41] Fendt S, Padmanabhan S, Blanch HW, Prausnitz JM. Viscosities of acetate or chloride based ionic liquids and some of their mixtures with water or other common solvents. J Chem Eng Data. 2011;56:31– 34.
[42] Swatloski RP, Spear SK, Holbrey JD, Rogers RD. Dissolution of cellulose with ionic liquids. J Am Chem Soc. 2002;124:4974– 4975.
[43] Zhang H, Wu J, Zhang J, He J. 1-Allyl-3-methylimidazolium chloride room temperature ionic liquid: A new and powerful nonderivatizing solvent for cellulose. Macromolecules. 2005;38:8272– 8277.
[44] Da Roz AL, Leite FL, Pereiro LV, Nascente PAP, Zucolotto V, Oliveira ON, Jr, Carvalho AJF. Adsorption of chitosan on spin-coated cellulose films. Carbohydrate Pol. 2010;80:65–70.
[45] Dreve S, Kacso I, Bratu I, Indrea E. Chitosan-based delivery systems for diclofenac delivery: Preparation and characterization. J Phys: Conference Series. 2009;182:1–4.
[46] Burns DA, Ciurczak EW. Handbook of Near-Infrared Analysis. Marcell Dekker; New York: 1992.
[47] Socrates G. Infrared characteristic group frequencies. John-Wiley; New York: 1994.
[48] Bettinetti G, Sorrenti M, Catenacci L, Ferrari F, Rosi S. Polymorphism, pseudopolymorphism, and amorphism of peracetylated α-, β-, and γ-cyclodextrins. J Parm Biomed Anal. 2006;41:1205– 1211.
[49] Ellis JW. Infra-red absorption by the N-H bond II in aryl, alkyl and aryl-alkyl amines. J Am Chem Soc. 1928;50:685–695.
[50] Miller CE. Chemical Principles of Near-Infrared Technology. In: Williams P, Norris K, editors. Near-Infrared technology in the agricultural and food industries. 2. American Association of Cereal Chemists; Minnesota, USA: 2001. pp. 19–37.
[51] Weber JW, Morris JC. Kinetics of adsorption of carbon from solution. J Sanit Eng Div Am Soc Civ Eng. 1963;89:31–39.

[52] Chakraborty S, Chowdhury S, Saha PD. Adsorption of Crystal Violet from aqueous solution onto NaOH-modified rice husk. Carbohydrate Polymers. 2011;86:1533– 1541.

[53] Gu W, Sun C, Liu Q, Cui H. Adsorption of avermectins on activated carbon: Equilibrium, kinetics, and UV-shielding. Trans Nonferrous Met Soc China. 2009;19:845– 850.

[54] Langmuir I. The constitution and fundamental properties of solids and liquids. J Am Chem Soc. 1916;38:2221–2295.

[55] Freundlich HMF. Over the adsorption in solution. J Phys Chem. 1906;57A:385– 471.

[56] Dubinin MM. The potential theory of adsorption of gases and vapours for adsorbents with energetically non-uniform surfaces. Chem Rev. 1960;60:235– 266.

[57] Dubinin MM, Radushkevich LV. The equation of the characteristic curve of the activated charcoal. Proc Acad Sci USSR Phys Chem Sect. 1947;55:331– 337.

[58] Chowdhury S, Chakraborty S, Saha P. Biosorption of Basic Green 4 from aqueous solution by Ananas comosus (pineapple) leaf powder. Colloids and surfaces B: Biointerfaces. 2011;84:520– 527.

Supplementary Material

SUPRAMOLECULAR COMPOSITE MATERIALS FROM CELLULOSE, CHITOSAN AND CYCLODEXTRIN: FACILE PREPARATION AND THEIR SELECTIVE INCLUSION COMPLEX FORMATION WITH ENDOCRINE DISRUPTORS

Simon Duri and Chieu D. Tran*

Department of Chemistry, Marquette University, P. O. Box 1881, Milwaukee, WI 53201

SUPPORTING INFORMATION

Analysis of Kinetic Data

The pseudo-first-order, pseudo-second-order and intra-particle diffusion kinetic models were used to evaluate the adsorption kinetics of different polychlorophenols and BPA and to quantify the extent of uptake in the adsorption process

Pseudo-first-order kinetic model

The linear form of Lagergren's pseudo-first-order equation is given as:[1]

$$\ln(q_e - q_t) = \ln q_e - k_1 t \qquad \text{[SI-1]}$$

where q_t and q_e are the amount of pollutant adsorbed at time t and at equilibrium (mg g^{-1}) respectively and k_1 (min^{-1}) is the pseudo first order rate constant calculated from the slope of the linear plot of ln ($q_e - q_t$) versus t.

Pseudo-second-order kinetic model

According to the Ho model, the rate of pseudo second order reaction may be dependent on the amount of species on the surface of the sorbent and the amount of species sorbed at equilibrium. The equilibrium sorption capacity, q_e, is dependent on factors such as temperature, initial

concentration and the nature of solute-sorbent interactions. The linear expression for the Ho model can be represented as follows:[1]

$$\frac{t}{q_t} = \frac{1}{k_2 q_e^2} + \frac{1}{q_e} t \qquad [SI-2]$$

where k_2 is the pseudo-second order rate constant of sorption (g/mg.min), q_e is the amount of analyte adsorbed at equilibrium (mg/g), q_t is the amount of analyte adsorbed at any time t (mg/g). If the initial adsorption rate h is

$$h = k_2 q_e^{\ 2} \qquad [SI-3]$$

Then Eq SI-2 can be rearranged as

$$\frac{t}{q_t} = \frac{1}{h} + \frac{1}{q_e} t \qquad [SI-4]$$

A linear plot can be obtained by plotting t/q_t against t. q_e and h, can obtained from the slope and intercept; k_2 can be calculated from h and q_e according to Eq SI-3.

Intra-particle diffusion model

The intra-particle diffusion equation is given as follows:[2,3]

$$q_t = k_i t^{0.5} + I \qquad [SI-5]$$

where k_i (mg g^{-1} $min^{-0.5}$) is the intra-particle diffusion rate constant and I (mg g^{-1}) is a constant that gives the information regarding the thickness of the boundary layer[2,3]. According to this model, if the plot of qt versus $t^{0.5}$ gives a straight line, then the adsorption process is controlled by intra-particle diffusion, while, if the data exhibit multi-linear plots, then two or more steps influence the adsorption process.

Analysis of Adsorption isotherms

Different isotherm models have been developed for describing sorption equilibrium. The Langmuir, Freundlich and Dubinin–Radushkevich (D–R) isotherms were used in the present study.

Langmuir isotherm. The Langmuir sorption isotherm describes that the uptake occurs on a homogeneous surface by monolayer sorption without interaction between adsorbed molecules and is commonly expressed as (Langmuir, 1916):[4]

$$\frac{C_e}{q_e} = \frac{C_e}{q_m} + \frac{1}{K_L q_m} \qquad \text{[SI-6]}$$

where q_e (mg g^{-1}) and C_e (mg L^{-1}) are the solid phase concentration and the liquid phase concentration of adsorbate at equilibrium respectively, q_m (mg g^{-1}) is the maximum adsorption capacity, and K_L (L mg^{-1}) is the adsorption equilibrium constant. The constants K_L and q_m can be determined from the slope and intercept of the plot between C_e/q_e and C_e.

Freundlich isotherm. The Freundlich isotherm is applicable to non-ideal adsorption on heterogeneous surfaces and the linear form of the isotherm can be represented as (Freundlich, 1906):[5]

$$\log q_e = \log K_F + \left(\frac{1}{n}\right) \log C_e \qquad \text{[SI-7]}$$

where q_e (mg g^{-1}) is the equilibrium concentration on adsorbent, C_e (mg L^{-1}) is the equilibrium concentration in solution, K_F (mg g^{-1}) (L g^{-1})$^{1/n}$ is the Freundlich constant related to sorption capacity and n is the heterogeneity factor. K_F and 1/n are calculated from the intercept and slope of the straight line of the plot log q_e versus log C_e. n value is known to be a measure of the favorability of the sorption process.[6] A value between 1 and 10 is known to represent a favorable sorption.

Dubinin–Radushkevich (D–R) isotherm. The Dubinin–Radushkevich (D–R) isotherm model envisages about the heterogeneity of the surface energies and has the following formulation:[7]

$$\ln q_e = \ln q_m - \beta\varepsilon^2 \qquad \text{[SI-8]}$$

$$\varepsilon = RT\ln\left(1+\frac{1}{C_e}\right) \qquad \text{[SI-9]}$$

where q_m (mg g^{-1}) is the maximum adsorption capacity, β (mmol^2 J^{-2}) is a coefficient related to the mean free energy of adsorption, ε (J $mmol^{-1}$) is the Polanyi potential, R is the gas constant (8.314 J mol^{-1} K^{-1}), T is the temperature (K) and C_e (mg L^{-1}) is the equilibrium concentration. The D–R constants q_m and β can be determined from the intercept and slope of the plot between ln q_e and ε^2.

The constant β in the D-R isotherm model is known to relate to the mean free energy E (KJ mol^{-1}) of the sorption process per mole of the analyte which in turn can give information about the sorption mechanism. E can be calculated using the equation 1 below.[8]

$$E = \frac{1}{\sqrt{2\beta}} \qquad \text{[SI-10]}$$

According to this theory, the adsorption process is supposed to proceed via chemisorb if E is between 8 and 16 KJmol^{-1}whereas for values less than 8 KJmol^{-1}, the sorption process is often governed by physical nature[8].

REFERENCES

(1) Chakraborty, S.; Chowdhury, S.; Saha, P. D. Adsorption of Crystal Violet from aqueous solution onto NaOH-modified rice husk. *Carbohydrate Polymers.* **2011,** 86, 1533 – 1541.

(2) Weber, J. W.; Morris, J. C. Kinetics of adsorption of carbon from solution. *J. Sanit. Eng. Div. Am. Soc. Civ. Eng.* **1963**, 89, 31-39.

(3) Gu, W.; Sun, C.; Liu, Q.; Cui, H. Adsorption of avermectins on activated carbon: Equilibrium, kinetics, and UV-shielding. *Trans. Nonferrous Met. Soc. China*. **2009,** 19, 845 – 850.

(4) Langmuir, I. The constitution and fundamental properties of solids and liquids. *J. Am. Chem. Soc.***1916,** 38, 2221 – 2295.

(5) Freundlich, H. M. F. Over the adsorption in solution. *J. Phys. Chem.* **1906,** 57A, 385 – 471.

(6) Chowdhury, S.; Chakraborty, S.; Saha, P. Biosorption of Basic Green 4 from aqueous solution by Ananas comosus (pineapple) leaf powder. *Colloids and surfaces B: Biointerfaces.* **2011,** 84, 520 – 527.

(7) Dubinin, M. M. Radushkevich, L. V. The equation of the characteristic curve of the activated charcoal. *Proc. Acad. Sci. USSR Phys. Chem. Sect.*, **1947,** 55, 331 – 337.

(8) Kundu, S.; Gupta, A. K. Arsenic adsorption onto iron oxide-coated cement (IOCC): regresssion analysis of equilibrium data with several isotherm models and their optimization. *Chem. Eng. J.* **2006,** 122, 96 – 106.

Table SI-1. Kinetic parameters for adsorption of Chlorophenols and BPA onto 100% CS film

		Pseudo first-order kinetic model				Pseudo second-order kinetic model			
Analyte	**qe, expt (M/g)**	**qe(M/g)**	**K_1 (min^{-1})**	**R^2**	**MSC**	**qe(M/g)**	**K_2 (M^{-1} min^{-1})**	**R^2**	**MSC**
2-ClPh	1.30E-03	1.48E-03	0.089	0.9865	3.305	1.32E-03	385.9	0.9998	8.02
3-ClPh	1.62E-03	3.25E-03	0.050	0.9745	2.669	1.68E-03	133.5	0.9960	5.21
4-ClPh	1.64E-03	6.49E-04	0.051	0.9849	2.861	1.66E-03	214.6	0.9996	7.52
3,4 Di-ClPh	2.23E-03	7.23E-04	0.048	0.8769	0.761	2.27E-03	169.8	0.9999	8.72
2,4,5 Tri-ClPh	1.05E-02	9.90E-03	0.016	0.9843	3.917	1.20E-02	2.1	0.9991	6.60
BPA	1.74E-03	5.88E-04	0.040	0.8947	1.680	1.80E-03	168.3	0.9995	7.24

Table SI-2. Kinetic parameters for adsorption of Chlorophenols and BPA onto 100% CEL film

		Pseudo first-order kinetic model				Pseudo second-order kinetic model			
Analyte	**qe, expt (M/g)**	**qe(M/g)**	**K_1 (min^{-1})**	**R^2**	**MSC**	**qe(M/g)**	**K_2 (M^{-1} min^{-1})**	**R^2**	**MSC**
2-ClPh	4.11E-04	1.45E-04	0.029	0.6469	0.041	3.93E-04	702.3	0.9871	3.95
3-ClPh	3.19E-04	4.95E-04	0.044	0.9747	2.678	3.20E-04	293.8	0.9822	3.72
4-ClPh	5.79E-04	1.69E-04	0.055	0.9559	1.788	5.81E-04	2054.2	0.9999	9.13
3,4 Di-ClPh	7.98E-04	9.44E-04	0.142	0.9665	2.397	8.19E-04	315.6	0.9996	7.47
2,4,5 Tri-ClPh	1.87E-03	1.01E-03	0.011	0.9714	3.287	1.95E-03	25.4	0.9967	5.32
BPA	7.27E-04	4.62E-04	0.014	0.9715	3.156	8.05E-04	78.9	0.9911	4.39

Table SI-3. Kinetic Parameters for Adsorption of Chlorophenols and BPA onto 50:50 CS:β-TCD Composite Material

		Pseudo first-order kinetic model				***Pseudo second-order kinetic model***			
Analyte	**q_e, expt (M/g)**	**q_e(M/g)**	**K_1 (min^{-1})**	**R^2**	**MSC**	**q_e(M/g)**	**K_2 (M^{-1} min^{-1})**	**R^2**	**MSC**
2-ClPh	7.30E-04	7.76E-04	0.058	0.9981	5.249	7.58E-04	268.4	0.9967	5.32
3-ClPh	1.22E-03	1.96E-03	0.041	0.9936	4.046	1.25E-03	118.6	0.9934	4.71
4-ClPh	9.64E-04	4.79E-03	0.119	0.9567	1.806	8.99E-04	313.1	0.9957	5.11
3,4 Di-ClPh	1.87E-03	1.45E-03	0.055	0.9636	2.647	1.99E-03	57.1	0.9978	5.77
2,4,5 Tri-ClPh	7.45E-03	7.92E-03	0.015	0.9548	2.861	8.84E-03	2.1	0.9996	7.41
BPA	1.42E-03	1.12E-03	0.028	0.9782	3.381	1.59E-03	37.6	0.9994	7.11

Table SI-4. Kinetic parameters for adsorption of Chlorophenols and BPA onto 50:50 CEL:β-TCD Composite Material

		Pseudo first-order kinetic model				Pseudo second-order kinetic model			
Analyte	**q_e, expt (M/g)**	**q_e(M/g)**	**K_1 (min^{-1})**	**R^2**	**MSC**	**q_e(M/g)**	**K_2 (M^{-1} min^{-1})**	**R^2**	**MSC**
2-ClPh	1.24E-03	8.70E-04	0.041	0.8960	1.597	1.30E-03	100.2	0.9975	5.57
3-ClPh	9.26E-04	5.55E-04	0.020	0.9410	2.259	9.87E-04	77.9	0.9964	5.33
4-ClPh	1.33E-03	1.04E-03	0.028	0.8161	1.122	1.41E-03	58.0	0.9993	6.93
3,4 Di-ClPh	8.71E-04	5.28E-04	0.047	0.9422	2.185	9.12E-04	160.6	0.9992	6.84
2,4,5 Tri-ClPh	1.92E-03	1.31E-03	0.021	0.9867	3.957	2.00E-03	33.2	0.9995	7.26
BPA	1.28E-03	7.93E-04	0.030	0.9291	2.147	1.34E-03	65.5	0.9987	6.28

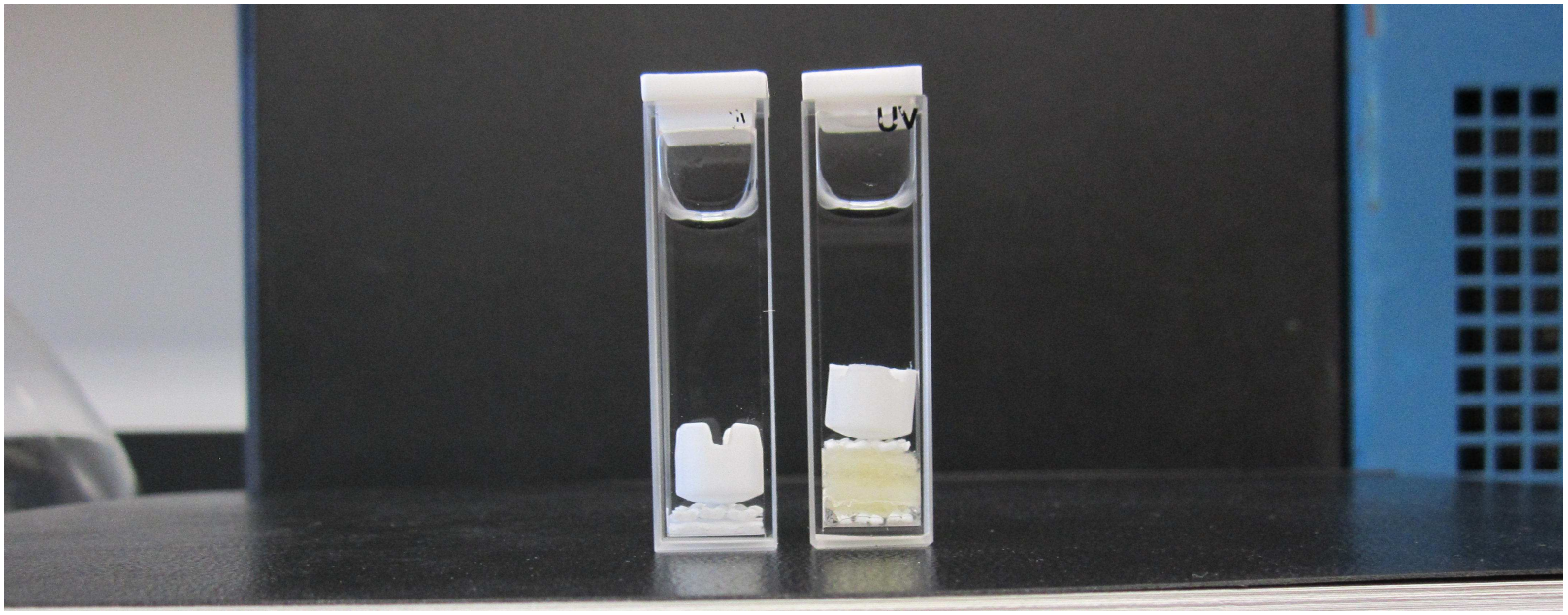

Figure SI-1. Photograph of two cells (sample cell (right) and blank (left) used to measure adsorption kinetics of the pollutants by the composite materials. See text for detail description.

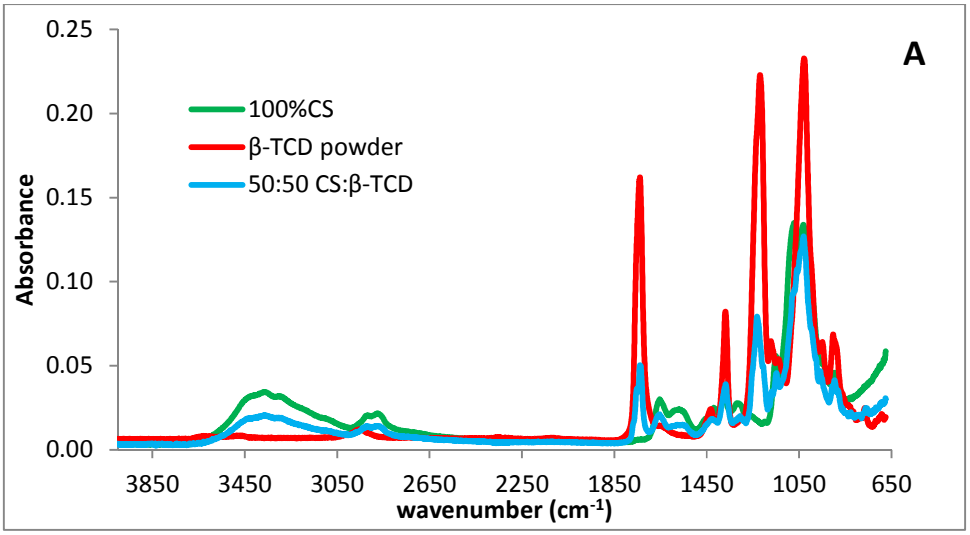

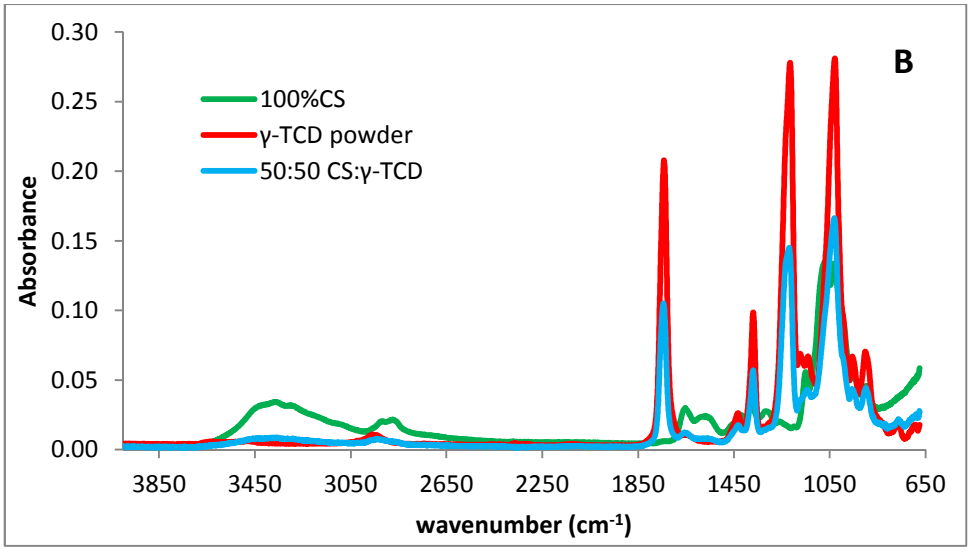

Figure SI-2. FTIR spectra of (A) 100%CS, β-TCD powder and 50:50 CS:β-TCD and (B) 100%CS, γ-TCD and 50:50 CS:γ-TCD

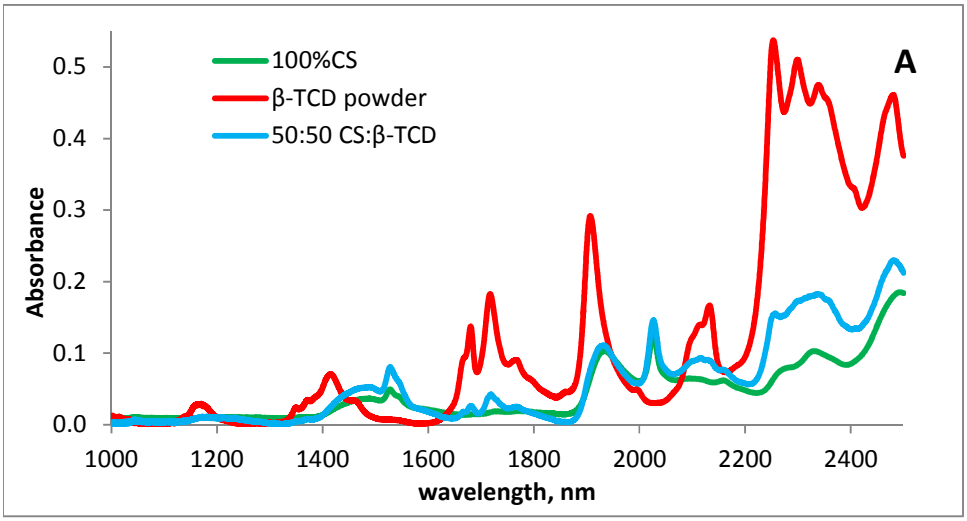

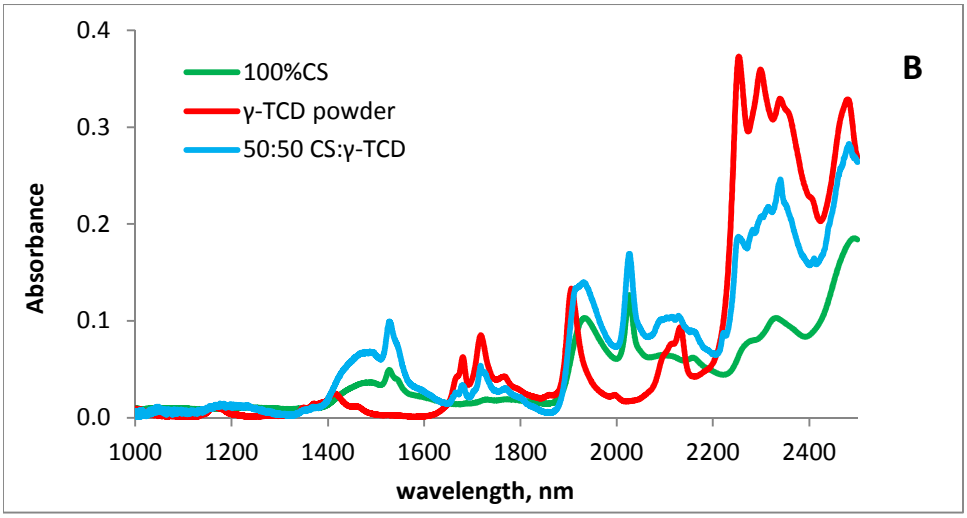

Figure SI-3. NIR spectra of (A) 100%CS, β-TCD powder and 50:50 CS:β-TCD and (B) 100%CS, γ-TCD and 50:50 CS:γ-TCD.

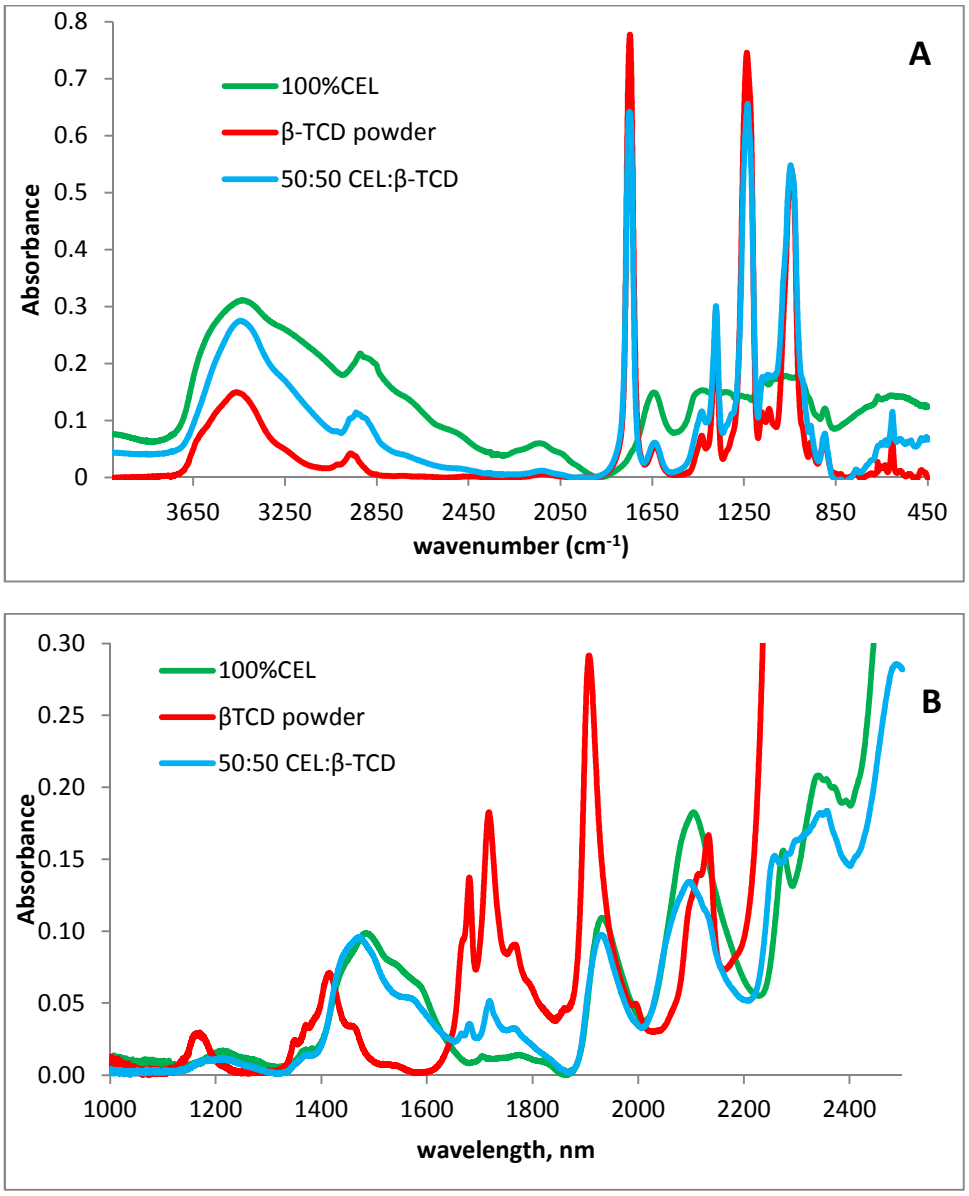

Figure SI-4. A) FT-IR and B) NIR spectra of CEL/TCD composite materials.

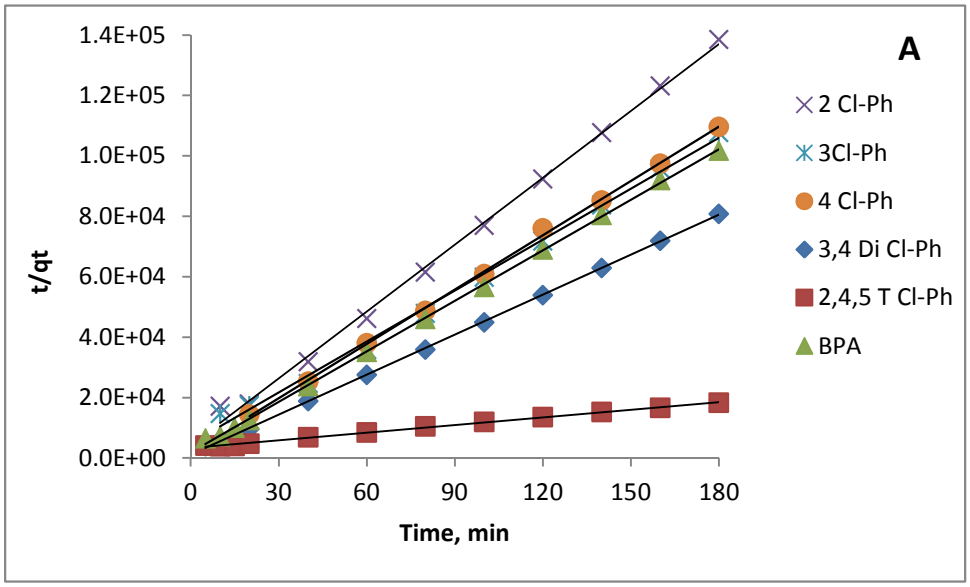

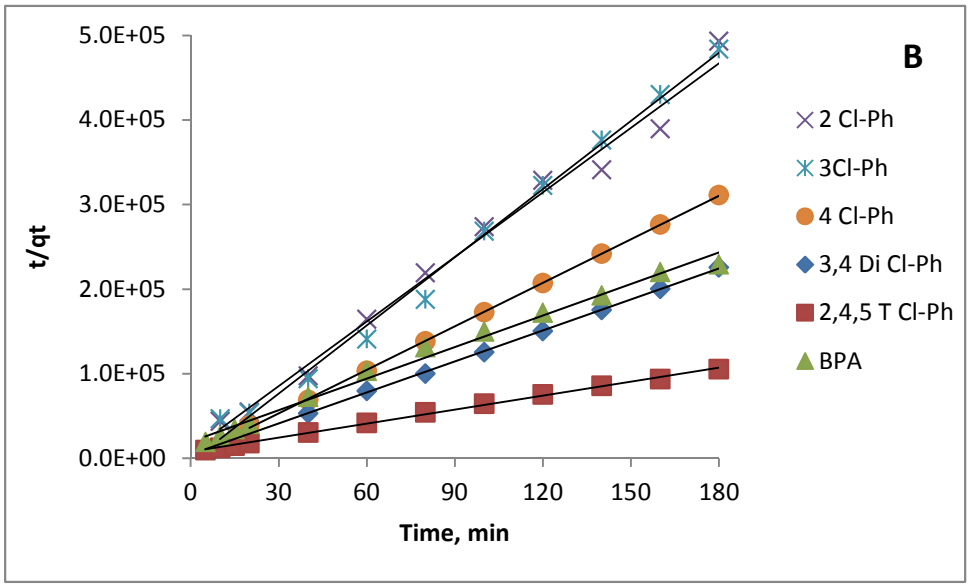

Figure SI-5: Pseudo second order linear plots for A) 100%CS and B) 100%CEL composite materials

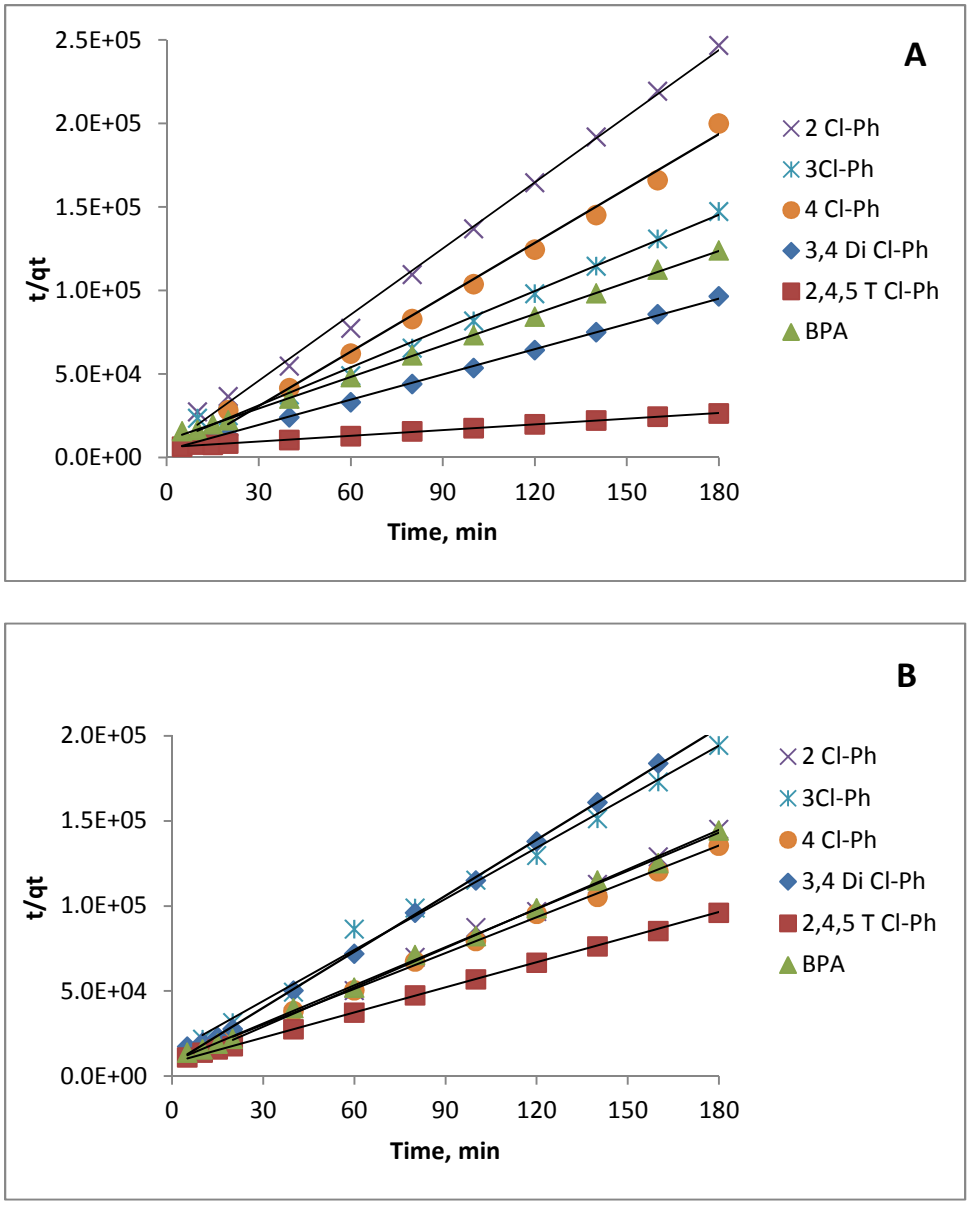

Figure SI-6: Pseudo second order linear plots for A) 50:50 CS:β-TCD and B) 50:50 CEL:β-TCD composite materials